universität wien

# MASTERARBEIT

Titel der Masterarbeit

„The role of myeloid PI3Kinase – pathway in tumor immune surveillance“

verfasst von

Leslie Hanz, BSc

angestrebter akademischer Grad

Master of Science (MSc)

Wien, 2015

| | |
|---|---|
| Studienkennzahl lt. Studienblatt: | A 066 877 |
| Studienrichtung lt. Studienblatt: | Masterstudium Genetik und Entwicklungsbiologie |
| Betreut von: | Ass.-Prov. Priv.-Doz. Mag. Dr. Gernot Schabbauer |

# Abstract

Myeloid cells, including phagocytes and antigen-presenting cells represent important parts of the innate immune system. Via the production of cytokines, the phagocytosis of microbes and the activation of further leukocytes, they are implicated in the resolution of inflammatory processes and tissue remodeling. One of the mechanism by which solid tumors evade the immune system, is the active recruitment of immune-suppressive, tolerogenic macrophages. It has been found that myeloid cells can contribute to tumor progression by undergoing phenotypical conversion from the "classically" activated inflammatory state (M1) to the "alternatively" activated tumor tolerating state (M2). The PI3K/PTEN signaling pathway plays an important role in this fate decision process, whereby myeloid PTEN-deficiency leads to a shift towards M2 polarization.

Phosphoinositide 3-kinases (PI3Ks) are an enzyme family involved in intracellular signal transduction. Signaling via PI3K has many downstream effects, including the promotion of cell survival and cell proliferation, the increase of glycolytic flux and the inhibition of apoptosis. Hyperactivation of the PI3K pathway by the deletion or inactivation of PTEN by germline- or somatic mutations is commonly observed in a variety of malignancies. These include different types of human cancer, making this pathway one of the most attractive targets for therapeutic intervention. Previous experiments have shown that myeloid PTEN-deficiency leads to an up-regulation of M2 marker genes, an enhanced expression of anti-inflammatory cytokines, as well as elevated levels of suppressive dendritic-cell subsets and regulatory T-cells. To investigate the role of the PI3K/PTEN pathway in tumor development, we chemically induced colitis-associated colon cancer (CAC) in myeloid PTEN-deficient mice. CAC describes colorectal tumor formation resulting from a previous state of inflammation, often due to inflammatory bowel disease. We used an AOM/DSS driven colorectal cancer mouse model to induce CAC in myeloid PTEN-deficient- and wild type mice, to examine the role of myeloid PI3K/PTEN in tumor formation and development. Previous experiments performed with naïve myeloid PTEN-deficient mice show a clear shift of myeloid cell polarization towards the immuno-suppressive M2 phenotype. Therefore we assume that hyperactivation of the PI3K pathway in myeloid cells, will lead to anti-inflammatory effects and enhanced suppression of anti-tumor immune responses in our CAC model. Thus we hypothesize that myeloid PTEN-deficiency will result in the up-regulation of immune-

suppressive myeloid cell subsets, hence leading to increased tumor formation and tumor burden in our CAC cancer model. To determine polarization of myeloid cells, we compared expression levels of M1 and M2 marker genes as well as secretion levels of pro- and anti-inflammatory cytokines, released from cells isolated from lymphoid organs, obtained from myeloid PTEN-deficient mice and wild type mice. Tumor formation and progression was assessed by the isolation of colonic tumors after the treatment period. Tumors were examined in size and weight and immune-histochemistry was performed to quantify tumor formation. Furthermore survival of wild type and knockout mice was evaluated during the AOM/DSS treatment period.

In line with our initial hypothesis, we found an up-regulation of various M2 marker genes and cytokines in cells isolated from myeloid PTEN-deficient mice. In line with these results, we were also able to show that not only the amount of tumors isolated from myeloid PTEN-deficient mice was higher compared to wild type mice, but also the relative tumor size was increased. Hence we found increased tumor burden in myeloid PTEN-deficient mice suffering from colitis-associated colon cancer, resulting in decreased survival.

# Zusammenfassung

Myeloide Zellen wie Phagozyten und Antigen-präsentierende Zellen sind wichtige Bestandteile des angeborenen Immunsystems. Durch die Produktion diverser Zytokine, die Phagozytose von Mikroben und die Aktivierung und Rekrutierung weiterer Leukozyten, sind sie ausschlaggebend für die Auflösung inflammatorischer Prozesse und die Einleitung Gewebs-remodellierender Vorgänge. Ein Mechanismus, der es Tumorzellen ermöglicht sich dem Immunsystem zu entziehen, ist die aktive Rekrutierung immunsupprimierender, tolerogener Makrophagen. Es konnte gezeigt werden, dass myeloide Zellen zur Tumorentwicklung beitragen können, indem sie eine phänotypische Umwandlung vom „klassisch" aktivierten inflammatorischen Zustand (M1) zum „alternativ" aktiviertem Tumor-tolerierenden Zustand (M2) durchlaufen. Der PI3K/PTEN Signalweg spielt eine wichtige Rolle in diesem Entscheidungsprozess, wobei myeloide PTEN Defizienz zu einer erhöhten M2 Polarisierung führt.

Phosphoinositide 3-Kinasen (PI3Ks) sind eine Enzymfamilie, die eine wichtige Rolle in der intrazellulären Signaltransduktion spielt. Signaltransduktion via PI3K fördert u.a. die Überlebensfähigkeit von Zellen, Zell-Proliferation, die Erhöhung glykolytischer Aktivitäten, sowie die Inhibierung der Apoptose. Eine Hyperaktivierung des PI3K Signalwegs, durch den Verlust oder die Inaktivierung von „Phosphatase and tensin homolog**"** PTEN (Antagonist von PI3K) durch Keimbahn Mutationen oder somatische Mutationen, tritt im Verlauf diverser Krankheiten auf. Mitunter betroffen sind verschiedene Arten von Krebs, was den PI3K Signalweg zu einem attraktiven Ziel für therapeutische Interventionen macht. Vorangegangene Experimente konnten zeigen, dass myeloide PTEN Defizienz zur Hochregulierung von M2 Markergenen, zur erhöhten Sekretion anti-inflammatorischer Zytokine und dem vermehrten Vorhandensein suppressiver dendritischer Zellsubtypen, sowie regulatorischer T-Zellen führt.

Um die Rolle des PI3K/PTEN Signalwegs im angeborenen Immunsystem während der Entstehung von Tumoren zu untersuchen, wurde Kolitis assoziierter Darmkrebs (engl.: colitis-associated colon cancer – CAC), chemisch in Mäusen mit myeloider PTEN Defizienz hervorgerufen. CAC beschreibt ein Krankheitsbild colorektaler Tumore, die durch vorhergehende Entzündungen (chronisch entzündliche Darmerkrankung – engl.: inflammatory bowl disease – IBD) entstehen.

Durch die Verwendung eines AOM/DSS induzierten Darmkrebsmodells in Mäusen mit myeloider PTEN Defizienz, soll die Rolle des PI3K/PTEN Signalwegs in der Tumorentstehung und Entwicklung untersucht werden.

Bereits in naiven Mäusen mit myeloider PTEN Defizienz durchgeführte Experimente, konnten eine Polarisationstendenz myeloider Zellen in Richtung des anti-inflammatorischen M2 Phänotyps zeigen. Wir gehen deshalb davon aus, dass eine myeloide Hyperaktivierung des PI3K Signaltransduktionswegs zu anti-inflammatorischen Effekten und verstärkter Unterdrückung der anti-Tumor Immunantwort in einem entzündungs-basierendem Darmkrebs Model führt. Dementsprechend glauben wir, dass die Hyperaktivierung von PI3K zu einer Hochregulierung immunsupprimierender myeloider Zellen und somit zu einer erhöhten Tumorbildung und Tumorlast in unserem Model führen wird.

Um die Polarisierung myeloider Zellen festzustellen, wurde die Expression diverser M1 und M2 Markergene, sowie die Ausschüttung pro- und anti-infammatorischer Zytokinen untersucht, welche aus Zellen lymphoider Organen isoliert wurden. Tumorraten wurden durch die Isolierung der Tumore nach der Behandlungsperiode untersucht, wobei die Tumore nach ihrer Größe und ihrem Gewicht analysiert wurden und die Größe der Tumore durch die Anwendung von Immunohistochemie quantifiziert wurde. Weiters wurden die Überlebensraten aller Wildtyp- und Knockout-Mäuse während der gesamten Behandlungsperiode ermittelt.

Entsprechend unserer ursprünglichen Annahme, haben wir eine Hochregulierung diverser M2 Markergene und Zytokine in Zellen, die aus myeloid PTEN-defizienten Mäusen isoliert wurden, gefunden. Wir konnten zeigen, dass sowohl die Größe, als auch die Anzahl der Tumore, welche aus Knockout-Mäusen isoliert wurden, höher ist als in Wildtyp-Mäusen. Dementsprechend konnten wir eine erhöhte Tumorlast und eine reduzierte Überlebensrate in Mäusen mit myeloider PTEN Defizienz nachweisen.

# List of content

# 1. Introduction

## 1.1 The gastrointestinal tract

The gastrointestinal tract can be divided into the upper and the lower gastrointestinal tract. The upper gastrointestinal tract includes the esophagus, the stomach and the duodenum, the latter representing the first section of the small intestine. The lower gastrointestinal tract is made up of the small and the large intestine. The small intestine can be further subcategorized into duodenum, jejunum and ileum whereas the large intestine comprises the cecum, colon, rectum and anal canal. The vermiform appendix is attached to the cecum.

### 1.1.1 The small intestine

The major function of the small intestine is the absorption of digestion products (e.g. carbohydrates, lipids, proteins, vitamins, etc.) via the intestinal mucosa into the bloodstream.

After exiting the stomach, the gastric chyme (semifluid mass of partly digested food) passes the pyloric valve into the duodenum where the bile duct ends. There pancreatic juice - produced by the pancreas - and bile - produced by the liver – is secreted. While bile emulsifies fats into micelles, the digestive enzymes in the pancreatic juice breakdown proteins, carbohydrates and lipids. The pancreatic juice also contains bicarbonate, which in combination with the secretion of Brunner's glands - also found in the duodenum - neutralizes the stomach acids contained in gastric chyme. Brunner's glands produce a mucus-rich alkaline secretion, which also contains bicarbonate and protects the duodenum from the acidic content of chyme.

In the jejunum, this is the midsection of the small intestine, the plicae circulares (transversally running folds of the mucous membrane) and villi, which increase the surface area of the small intestine, absorb sugars, amino acids, fatty acids and other products of digestion into the bloodstream. Other remaining nutrients, as well as vitamin B12 and bile acid are absorbed in the last part of the small intestine, the ileum, which also contains villi.

### 1.1.2 The large intestine

Through the cecum which is the beginning of the large intestine, chyme from the ileum is passed to the colon. The colon can be further subdivided into the ascending colon, the transverse colon and the descending. The main function of the large intestine is to absorb water and salt from the solid wastes before they are eliminated from the body. It is also the side of bacterial fermentation of unabsorbed material.

### 1.1.3 The intestinal epithelium

The inner surface of the intestine is lined by a simple epithelium, representing the most rapidly self-renewing tissue in adult mammals, with a turnover rate of three to five days in mice (Barker et al., 2007; Makarenkova et al., 2006).

The epithelial layer of the proximal region of the intestine (the small intestine) is organized into crypts and villi, whereas latter are specialized in the absorption of micronutrients, while the distally located colon consists of crypts only which are mostly responsible for the compaction of stool.

The different cell types of the intestine are organized in a distinct pattern, which is similar in both the small and the large intestine. The base of each crypt is dedicated to the stem cell compartment, the transient-amplifying (TA) compartment is located in the middle portion of the crypts, and the differentiation zone expands from the middle part of the crypt to the tip of the villus. While the stem cells divide approximately once a day, their progeny (the transient-amplifying cells) is amplified through a series of rapid divisions. These TA cells then migrate up, whereby they differentiate. Depending on distinct transcription factors promoting one cell type but repressing another, cells end up as one of six different cell types found in the intestinal epithelium.

The vast majority of cells will differentiate into enterocytes or goblet cells. While enterocytes absorb nutrients from the intestinal lumen, goblet cells are responsible for mucus secretion. Tuft cells are believed to release Prostanoids into the intestinal lumen, whereas enteroendocrine cells secrete different hormones. Microfold cells (M cells) are located right above Peyer's patches where they transport antigen to antigen presenting cells situated in

intraepithelial pockets. Finally Paneth cells are found at the crypt base where they nurture intestinal stem cells (ISCs) and secrete antimicrobial products (Clevers and Batlle, 2013) (see Figure 1).

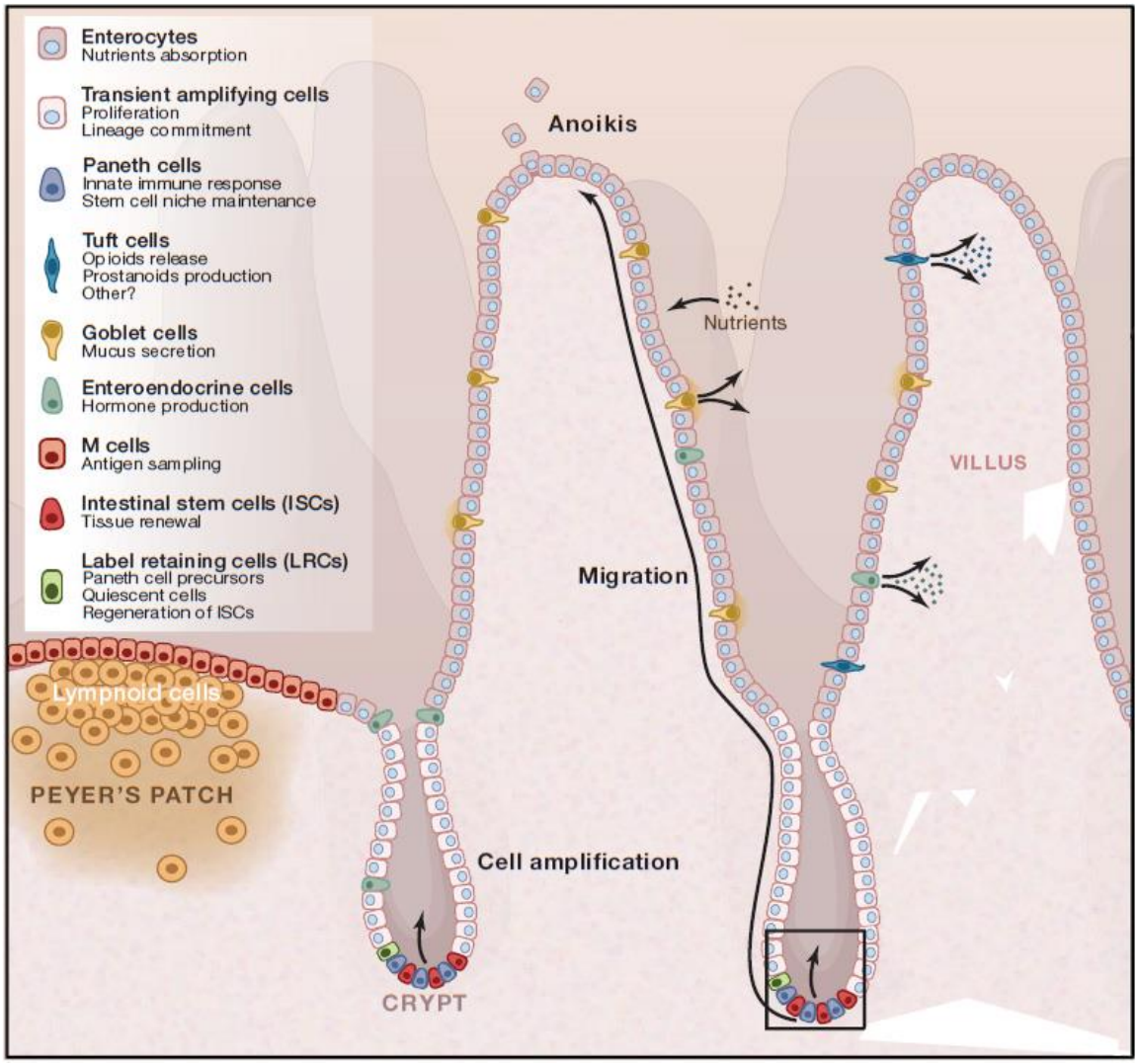


**Figure 1. The intestinal epithelium (modified from Clevers and Batlle 2013)**

Through the division of ISCs located at the crypt base, daughter cells are produced which migrate up towards the tip of the individual villus. These so called transient-amplifying cells will end up as one of six different cell types present in the intestinal epithelium. During their migration they become more and more committed to one of these cell types, via the expression of certain transcription factors. The most abundant cell types are enterocytes (adsorptive cells) and goblet cells (mucus-secreting cells). Other cell types include secretory cells like enteroendocrine cells which produce different hormones and tuft cells which are thought to produce prostanoids. Further on epithelial cells called Microfold cells (M cells) are located near Peyer's patches to transport antigen to antigen presenting cells situated in intraepithelial pockets. The sixth cell type found in the intestinal epithelium is called Paneth cells and is located at the crypt base where they nurture intestinal stem cells (ISCs) but also secrete antimicrobial substances.

## 1.2. Inflammation and Colon Cancer

It has been known for a long time that there is a well-established connection between inflammation and tumorigenesis. In the case of colorectal cancer (CRC), Inflammatory Bowel Disease (IBD) poses a great risk factor for the development of CRC, in this case termed colitis-associated colon cancer (CAC) (Terzić et al., 2010).

### 1.2.1 Inflammatory bowel disease

The term 'Inflammatory Bowel Disease' describes chronic inflammatory conditions of the mucosa of the colon and the small intestine, with Crohn's disease and ulcerative colitis being the major representatives of this disease (Podolsky, 2002). The risk of developing CAC within 30 years of suffering from IBD is higher than 20%, making IBD a major risk factor for the development of CRC (Lakatos and Lakatos, 2008).

### 1.2.2 Development of colorectal- and colitis-associated colon cancer

Both hereditary as well as environmental factors can contribute to the first step of tumorigenesis. The activation of various oncogenes and the inactivation of tumorsuppressors, caused by DNA mutations, are among the first steps of neoplasia. Tumorformation is a multistep process and malignant tumors arise from the accumulation of several mutations required for cancerogenesis (Fearon and Vogelstein, 1990).

In comparison with normal colonic epithelial tissue, which arises from various stem cells, colorectal tumors have a monoclonal composition, meaning that a tumor can arises from a single cell through clonal expansion (Fearon et al., 1987).

While mutations in epithelial cells or stem cells occur at random in various genes, mutations affecting the tumor suppressor adenomatous polyposis coli (APC) are upon the most frequently occuring mutations to form tumors. This results in activation and nuclear localisation of ß-Catenin (see Figure 2). The increased localisation of ß-Catenin to the

nucleus, can lead to uncontrolled cell proliferation. By binding to ß-Catenin, APC hinders the protein from translocation to the nucleus where it regulates cellular signaling events (Rubinfeld et al., 1993). Mutations in APC and ß-Catenin are typically early events in cancerogenic pathways. APC is usually proteolytically degraded as a result of active Wnt signaling, leading to the activation of ß-Catenin and its translocation to the nucleus (Morin et al., 1997).

One of the earliest changes found in the colon during the development of colorectal cancer, is the formation of aberrant crypt foci (ACF). APC mutation and the resulting activation of ß-Catenin is a requirement for ACF formation by leading to the transition of preneoplastic cells to ACF (Fearon and Vogelstein, 1990).

Crypt stem cells, which represent the cells of origin of colon cancer that are affected by APC mutations are no longer able to migrate to the tip of the individual villus and differentiate on their way up to the edge of the crypt where they are usually shed. This gives the premalignant cells time to acquire subsequent second and third mutations required for malignant conversion (Barker et al., 2009). However APC mutations are not necessarily essential in order to activate ß-Catenin. Mutations in glycogen synthase kinase-ß (GSK3-ß) and ß-Catenin itself can lead to the activation of ß-Catenin (Schneikert and Behrens, 2007). A study of *Helicobacter pylori*-induced gastric tumors has shown that pro-inflammatory signaling by TNF-α can lead to the activation and nuclear localization of ß-Catenin, without APC mutations (Oguma et al., 2008).

In addition, activation of the NF-κB and the Akt pathway by pro-inflammatory signaling can lead to ß-Catenin activation and nuclear localisation. Through the accumulation of additional mutations (e.g. activation of the oncogene K-ras and B-Raf, inactivation of diverse tumor suppressors including the TGF-ß receptor, activin receptors, p53 etc.) leading to the deregulation of different pathways, ACF can progress to adenomas and finally carcinomas, by the up-regulation of cyclooxygenase 2 (COX2) (Biswas et al., 2004; Grady and Carethers, 2008; Gupta and Dubois, 2001; Oshima et al., 1996; Takaku et al., 1998).

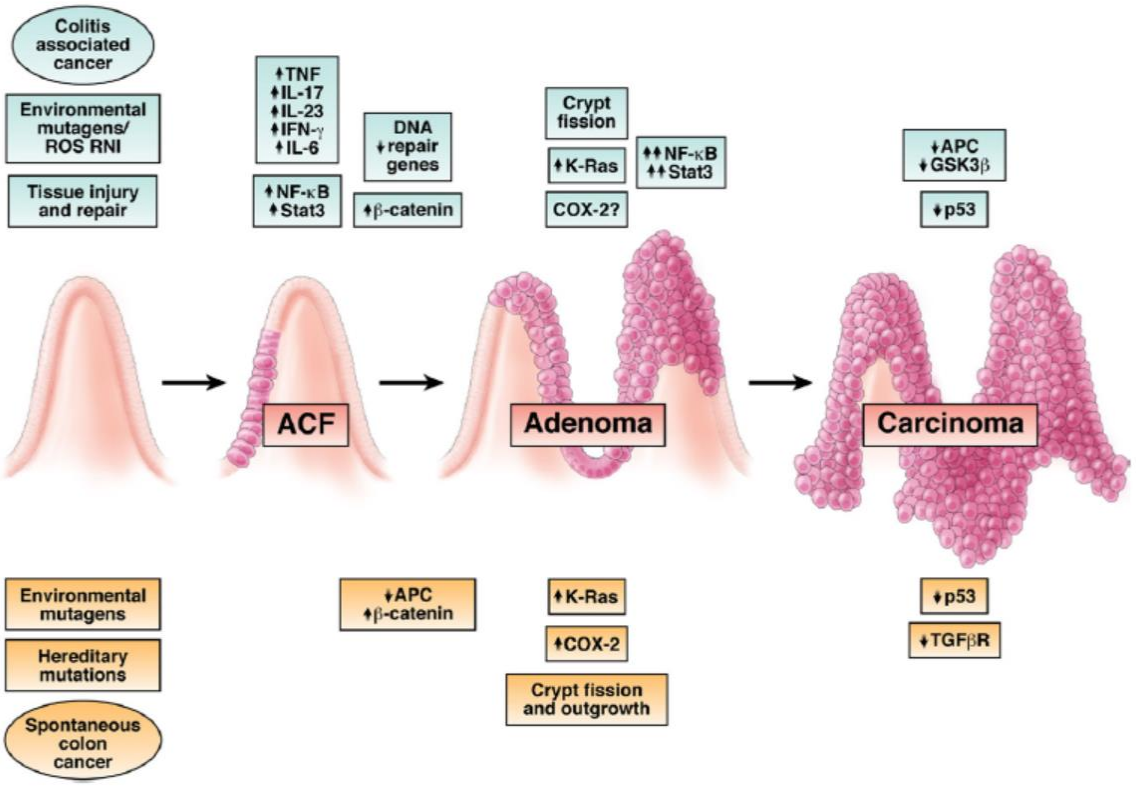


**Figure 2. Mechanisms of CRC and CAC development - (Terzić et al., 2010)**

Changes leading to the formation of CAC are depicted in blue, underlying mechanisms of CRC development are highlighted in yellow. An accumulation of mutations in tumor suppressor genes and oncogenes, some of which leading to the activation ß-Catenin signalling causes the transition of single preneoplastic cells to aberrant crypt foci (ACF) in CRC. Further mutations lead to the formation of adenomas and finally colorectal carcinomas. The secretion of proinflammatory cytokines in CAC leads to the mutations in oncogenes and tumor suppressor genes. Persistent inflammation then facilitates tumor promotion by activating proliferation and antiapoptotic properties of premalignant cells.(Terzić et al., 2010)

### 1.2.3 The role of the immune system in colon cancer

It is well established that colorectal and colitis-associated tumors are infiltrated by various cell types belonging to both the innate- and the adaptive immune system. Whereas cells of the adaptive immune system recruited to colonic tumors mostly comprise T-cells, a wide variety of innate immune cells is recruited to colorectal and colitis-associated tumors. Innate immune cells found in the proximity of colonic tumors include neutrophils, natural killer (NK) cells, dendritic cells (DC), mast cells and macrophages, especially tumor-associated macrophages (Atreya and Neurath, 2008). Furthermore, a heterogeneous population of

myeloid CD11b+ Gr1+ precursor cells, called myeloid-derived suppressor cells (MDSCs) with the ability to suppress T-cells and alter the cytokine expression profile of macrophages, is recruited by advanced tumors where they dampen anti-tumor immune responses (Gabrilovich and Nagaraj, 2009; Kusmartsev et al., 2004; Sinha et al., 2007). Furthermore, MDSCs are involved in the promotion of angiogenesis, metastasis and tumor cell-invasion (Gabrilovich and Nagaraj, 2009). Whereas in healthy patients, myeloid precursor cells, called immature myeloid cells (IMCs) are generated in the bone marrow, followed by their differentiation into macrophages, dendritic cells and granulocytes. However under pathological conditions, including cancer, sepsis, various infectious diseases, trauma, bone marrow transplantation and various autoimmune diseases a partial blockage of this differentiation can occur, as factors produced by the tumor's microenvironment promote the accumulation of IMCs to these sides, prevent their differentiation and promote their activation. The expansion and activation of these cells can then lead to an up-regulation of immune suppressive factors including arginase-1 and nitric oxide synthase (iNOS) (Gabrilovich and Nagaraj, 2009).

Whereas in sporadic CRC a balance between tumor-promoting inflammation and tumor immunesurveillance (through the role of CD8+ and CD4+ cells and NK cells) is mostly observed, the role of the immune system in CAC seems to be primarily pro-tumorigenic, through the role of innate immune cells, B cells and various T cell subtypes (Terzić et al., 2010).

### 1.2.4 AOM/DSS induce colitis-associated colon cancer

Colorectal cancer (CRC) is one of the most frequently occurring types of cancer, not related to smoking, in developed countries, with more than one million new cases being diagnosed each year. Despite of sporadic colorectal cancer, colitis-associated colon cancer (CAC), is probably the most serious complication in patients suffering from inflammatory bowel disease (IBD), a term uniting ulcerative colitis (UC) and Crohn's disease (CD) (Eaden et al., 2001; Tenesa and Dunlop, 2009; van Hogezand et al., 2002).

In order to simulate colitis-associated colon cancer in a mouse model, to provide pathophysiological insights into the disease, we used a well established model to mimic

inflammatory bowel disease by the use of dextran sodium sulfate (Okayasu et al., 1990; Seril et al., 2002). DSS is toxic to colonic epithelial cells and colitis is triggered by chemical disruption of the mucus layer that usually protects the colonic epithelial tissue and prevents direct contact of the intestinal mucosa with luminal microbiota. By causing defects in the barrier integrity of colonic epithelial cells (through the loss of components of tight junction complexes), larger molecules, including microbes present in the colonic lumen can now enter surrounding tissue, resulting in the recruitment and infiltration of innate immune cells, eliciting an overwhelming immune response (Johansson et al., 2010). DSS treatment results in weight loss, shortening of the colon as well as diarrhea. Combined with a pretreatment of a single injection of the genotoxic colonic carcinogen Azoxymethane (AOM), which causes DNA damage by alkylation, this treatment leads to colitis-associated colon cancer. Therefore AOM is injected into the intraperitoneal cavity of mice, followed by three cycles of DSS administration, by dissolving DSS into the mice's drinking water.

## 1.3 The PI3K and PTEN signaling pathway

Phosphoinositide 3-kinases (PI3Ks) are a family of heterodimeric enzymes, involved in intracellular signal transduction. Based on their primary structure, substrate specifity and regulation, three classes of PI3Ks can be distinguished. Most studies focus on class I family members which have been studied extensively, contrary to class II and III family members. This study also focuses on class I family members which can be further divided into class IA being the major PI3K group, and class IB subclasses (Gunzl and Schabbauer, 2008).

Class IA family members consist of a regulatory subunit (p85) and a catalytic subunit (p110). In quiescent cells, the catalytic subunit is kept in a low-activity state by p85. Through direct interaction with phosphotyrosine residues of activated receptors, p85 mediates the activation of the catalytic subunit p110 (Cantley, 2002).

Class IA PI3Ks are activated by receptor tyrosine kinases (RTKs) or adaptor proteins respectively (e.g. in the case of Toll-like receptor (TLR)-mediated PI3K activation) (Günzl and Schabbauer, 2008).

The pathway is activated via the binding of the ligand to the receptor (see Figure 3). In response to these extracellular signals (growth factors, hormones, antigen, etc.), the receptor tyrosine (Y) kinases are activated and undergo autophosphorylation. The regulatory subunit p85 harbours 2 Src homology 2 (SH2) domains which enable p85 to bind to phosphorylated tyrosine residues. Via the binding of the regulatory subunit p85 (via its SH2 domain) to phosphorylated Y residues of the activated receptor, the catalytic subunit p110 is recruited to the membrane where it converts phosphatidylinositol 4,5-bisphosphate [$PI(4,5)P_2$] to phosphatidylinositol 3,4,5-triphosphate [$PI(3,4,5)P_3$] by phosphorylation of phosphatidylinositol 4,5-bisphosphate at the D-3 position of the inositol ring (Worby and Dixon, 2014). Whereas in vivo, class I PI3Ks prefer $PI(4,5)P_2$ as their preferential substrate, they seem to be able to utilize PI, PI(4)P, or $PI(4,5)P_2$ in vitro (Vanhaesebroeck et al., 2001).

PI3K class II and III family members have different phosphatidylinositol (PtdIns) substrates (Gunzl and Schabbauer, 2008).

Various signaling proteins contain domains which specifically bind to D-3 phosphorylated phosphoinositides, including proteins containing pleckstring homology (PH) domains (various signaling proteins like serine – threonine kinases, protein tyrosine kinases and exchange

factors that regulate heterotrimeric guanosine triphosphate (GTP) – binding proteins (G proteins). These proteins are located in the cytosol of unstimulated cells and accumulate at the membrane upon lipid phosphorylation through the binding to PIP3 via their PH domain. Thereby different PH-domain - containing proteins, including important survival kinases such as AKT and its activating kinase phosphoinositide-dependent kinase 1 (PDK1), are recruited to the membrane by PIP3. The association with PIP3 brings the protein serine-threonine kinase AKT (also called protein kinase B (PKB)) in proximity with PDK1 at the membrane, leading to phosphorylation of AKT by PDK1 (Cantley, 2002).

Catalytically active AKT is able to phosphorylate a number of host proteins which can lead to diverse downstream effects, including promotion of cell proliferation and survival, increase of cellular glycolytic flux as well as inhibition of apoptosis (Worby and Dixon, 2014).

One of the targets of AKT is the Forkhead-related transcription factor 1 (FKHR-L1). Its phosphorylation by AKT creates a binding site for proteins of the 14-3-3 family. Resulting complexes of FKHR-L1 and 14-3-3 are retained in the cytosol, preventing FKHR-L1 to act as a transcription factor for various genes.

In the same manner, AKT creates a binding site for 14-3-3 proteins through phosphorylation of Bad, one of its other target proteins. The association with 14-3-3 proteins prevents Bad from binding to Bcl-2 family members Bcl-2 and Bcl-XL which can then trigger a cell survival response.

Phosphorylation of glycogen synthase kinase 3 (GSK3), another target of AKT, turns off the catalytic activity of this enzyme, resulting in the activation of pathways that are normally repressed by GSK3. GSK3 is constitutively active in unstimulated cells where it phosphorylates different proteins (glycogen synthase, c-Myc, cyclin D, etc.), to keep them in an inactive state or to promote their degradation (Cantley, 2002).

The phosphatase and tensin homolog deleted on chromosome 10 (PTEN) has dual protein and lipid phosphatase activity, whereas the potential to dephosphorylate protein targets is limited.

Via its lipid phosphatase activity it antagonizes the function of PI3K by catalyzing the reverse reaction from PIP3 to PIP2, thereby acting as a tumor suppressor by negatively regulating the PI3K – AKT – mTOR pathway. The decrease of PIP3 at the membrane also leads to a decrease in AKT signaling as PIP2 is inert and is not able to attract signaling proteins to the

membrane. Thereby PTEN negatively regulates PI3K/AKT signaling, leading to decreased phosphorylation of AKT substrate. The decrease in AKT signaling results in alterations of cell signaling, cell cycle progression, metabolism, migration, apoptosis, transcription and translation (Hollander et al., 2011).
The importance of PI3K/AKT signaling is underlined by the fact that PTEN is among the most frequently inactivated tumor suppressor genes in many types of cancer (Hollander et al., 2011).

Whereas PTEN dephosphorylates the 3 position of $PI(3,4,5)P_3$ to produce $PI(4,5)P_2$, the termination of PI3K signaling can also be mediated by Src-homology 2 (SH2)-containing phosphatases (SHIP1 and SHIP2), which dephosphorylate the 5 position of the inositol ring resulting in $PI(3,4)P_2$.
$PI(3,4)P_2$ can still mediate some PI3K-dependent responses, but it impairs some downstream signaling of PI3K. However PTEN-deficiency, leading to enhanced PI3K signaling activity cannot be restored by endogenous SHIP phosphatase activity (Gunzl and Schabbauer, 2008).
SHIP2 seems to play an important role concerning the regulation of PI3K signaling downstream of insulin, as its loss causes a dramatic increase in insulin sensitivity (Cantley, 2002).

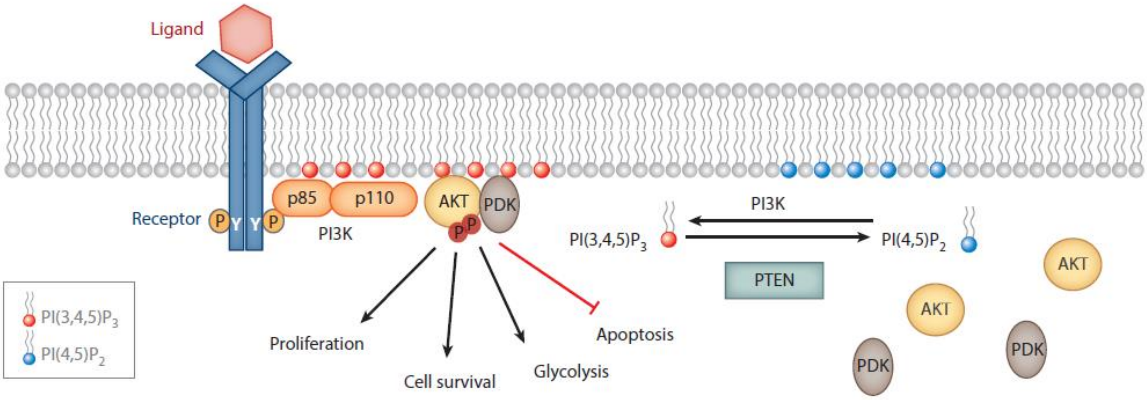


**Figure 3. The PI3K/PTEN pathway (Worby and Dixon, 2014)**

The pathway is activated via the binding of the ligand (growth factor, hormone, antigen, etc.) to the receptor. Upon this interaction the receptor tyrosin (Y) kinases are activated and undergo autophosphorylation. The regulatory subunit of PI3K (p58) is able to bind to the phosphorylated tyrosin residues and further recruits the catalytic subunit of PI3k (p110) to the membrane which than converts phosphatidylinositol 4,5-bisphosphate $PI(4,5)P_2$ to phosphatidylinositol 3,4,5-triphosphate $PI(3,4,5)P_3$ by phosphorylation of phopsphatidylinositol 4,5-bisphosphate at the D-3 position of the inositol ring. Proteins containing pleckstring homology (PH) domains and other signalling proteins specifically bind to D-3 phosphorylated phosphoinositides. Consequently PIP3 is able to recruit various signalling proteins including important survival kinases such as AKT and its activating kinase PDK1 to the membrane allowing AKT to trigger its downstream effects like promotion of cell proliferation and survival, increase of cellular glycolytic flux as well as inhibition of apoptosis. The phosphatase and tensin homolog deleted on chromosome 10 (PTEN) antagonizes the function of PI3K by catalyzing the reverse reaction from PIP3 to PIP2, thereby also decreasing the amount of AKT signalling.

## 1.4 Myeloid cell plasticity

Due to the heterogeneity and plasticity of functional stages, cells of the myeloid lineage exhibit a wide variety of different phenotypes, resulting from their ability to adapt one of a plethora of different polarization states. Recognition of environmental signals, e.g. derived from microbes, damaged tissue and resting or activated lymphocytes results not only in the activation of myeloid cells (e.g. macrophages), but also in the reshaping of subsequent responses to microbial encounters, leading to the reprogramming of the myelo-monocytic cell, a process termed “adoptive responses”. This shaping of mononuclear phagocytes plays an important role in their ability to adapt to their different functions. This means that phagocyte-mediated innate immunity exhibits an adaptive component, a property usually associated with the adaptive immune system, in response to microbial encounters (Bowdish et al., 2007).

Macrophages can be activated by the recognition of microbial products such as Lipopolysaccaride (LPS). The recognition itself can lead to alterations in the repertoire of pattern recognition receptors, including fluid-phase-pattern-recognition molecules such as molecules of the collectin family e.g. mannose-binding-lectins, as well as members of the pentraxin family, after the encounter of microbial moieties, hence reshaping subsequent responses in terms of phagocytosis and cytokine production (Bottazzi et al., 2010).

Due to the great overlap in surface marker expression, several macrophage subsets with distinct functions have been described (Geissmann et al., 2010).

Tumor associated macrophages (TAMs) which generally suppress anti-tumor immunity, are recruited to the tumor by various cytokines and chemokines produced by tumor cells and are mostly implicated in immunological tumor promoting responses. Depending on the tumors' microenvironment, the fate of the recruited macrophages is determined (Mantovani et al., 2008b).

Similar to the polarization of T helper cells (T helper type 1 and T helper type 2 cells), two distinct polarization states have previously been described for macrophages, namely the M1 classically activated macrophage and the M2 alternatively activated macrophage phenotype. These two phenotypes are discriminated from each other by the expression of different surface markers, distinct gene expression levels, as well as secretion levels of different

cytokines and chemokines. Depending on these markers, a multitude of different macrophage polarization stages can be discriminated, between the two extremes, the M1 and the M2 phenotype (Gordon and Taylor, 2005). Polarization towards the M1 phenotype is driven mainly via signal transducer and activator of transcription 1 (STAT1) signaling, whereas the M2 polarization is caused by signaling via STAT6 (Sica and Mantovani, 2012). M1 stimuli such as LPS and Interferon-γ (IFNγ) signal through the Toll like receptor 4 (TLR4), Interferon (IFNα) or IFNß receptor and IFNγ receptor pathways, which induces the activation of downstream transcription factors including nuclear factor kappa-light-chain-enhancer of activated B-cells consisting of p65 and p50 (NF-κB), activator protein-1 (AP-1), interferon regulatory factor 3 (IRF3) and STAT1, which leads to the transcription of M1 genes. M2 stimuli like Interleukin-4 (IL-4) and IL-13 signal through Interleukin-4 receptor α (IL-4Rα) to activate STAT6, which regulates the expression of M2 genes (Biswas and Mantovani, 2010).
Previous experiments have shown that macrophages contribute to tumor progression by undergoing phenotypical conversion from the M1 pro-inflammatory, to the M2 tumor tolerating state through the influence of the tumors' microenvironment.

### 1.4.1 The classically activated macrophage phenotype (M1)

The M1 macrophage or classically activated macrophage phenotype is characterized by a high expression of pro-inflammatory cytokines, such as Interleukin-23 (IL-23), tumor necrosis factor (TNF) and Interleukin-12 (IL-12), production of high amounts of reactive nitrogen- and reactive oxygen intermediates (RNI, ROI) as well as the promotion of T helper type 1 ($T_H1$) cell responses (see Figure 4a). M1 macrophages are associated with the defense against bacteria and viruses and in tumor destruction, which usually goes along with tissue damage. Compared with the M2 macrophage phenotype, M1 macrophages represent the more effective antigen-presenting cells due to their high expression of major histocompatibility complex class II and costimulatory molecules, whereas M2 macrophages show more phagocytic activity compared to M1 cells (Biswas and Mantovani, 2010; Gordon and Taylor, 2005; Mantovani, 2008).
Microbial products such as LPS and the $T_H1$ cytokine IFNγ have been shown to polarize macrophages towards the M1 phenotype.

Pattern recognition receptors (e.g. toll-like-receptors) enable macrophages to recognize pathogen associated molecular patterns (PAMPs) shared by entire groups of microbes. When a microbe binds to a phagocytosis receptor on the surface of a macrophage, the bound microbe can get ingested into a vesicle via the process of phagocytosis. Upon the ingestion, macrophages produce and secrete IL-12 which stimulates Natural Killer (NK) cells and T helper cells to secrete IFNy which in turn activates the macrophage. Activated macrophages then up-regulate reactive nitrogen- and reactive oxygen intermediates, as well as lysozymal enzymes, in order to kill the ingested microbe. They secrete pro-inflammatory cytokines and present antigen to T helper type 1 cells.

M1 and M2 macrophages also exhibit distinct chemokine profiles, with M1 cells expressing $T_H1$ attracting chemokines such as CXCL9 and CXCL10, thereby driving the polarisation and recruitment of $T_H1$ cells, hence amplifying the $T_H1$ response (Mantovani, 2008; Mantovani et al., 2004; Martinez et al., 2006).

### 1.4.2 The alternatively activated macrophage phenotype (M2)

In comparison to M1 macrophages, M2 or alternatively activated macrophages show an immune-suppressive, tumor-tolerating phenotype. They decrease inflammation and encourage tissue repair, wound healing as well as angiogenesis (via the release of pro-angiogenic growth factors such as Interleukin-8 (IL-8), VEGFA, VEGFC and EGF) and promote $T_H2$ responses (see Figure 4b). They are involved in the defense against intracellular parasites and in immune-regulatory functions. They are characterized by the up-regulation of certain marker genes (e.g. Fizz1, Arg1, Ym1) as well as high levels of secreted IL-10, the IL-1 decoy receptor and IL-1RA. They show high expression of scavenging, mannose and galactose receptors and produce ornithine and polyamines through the arginase pathway and are further characterized by low expression levels of IL-12 (Gordon and Taylor, 2005; Mantovani et al., 2002).

The $T_H2$ cytokine Interleukin-4 (IL-4) and Interleukin-13 (IL-13) polarizes macrophages towards the M2 alternatively activated phenotype, for example during helminth infections and allergy (Raes et al., 2005). Many other cytokines, including Interleukin-33 (IL-33), a cytokine of the IL-1 family are associated with $TH_2$ and M2 polarization respectively. IL-33

has been shown to amplify IL-13 driven polarization of alveolar macrophages towards the M2 phenotype (Hazlett et al., 2010).

M2 macrophages express CCL17, CCL22 and CCL24, the corresponding receptors (CCR4, CCR3) are present on $T_{reg}$ cells, $T_H2$ cells, eosinophiles and basophiles, therefore the secretion of these chemokines leads to the recruitment of these cells and polarized, $T_H2$ cell response (Mantovani, 2008; Mantovani et al., 2004; Martinez et al., 2006).

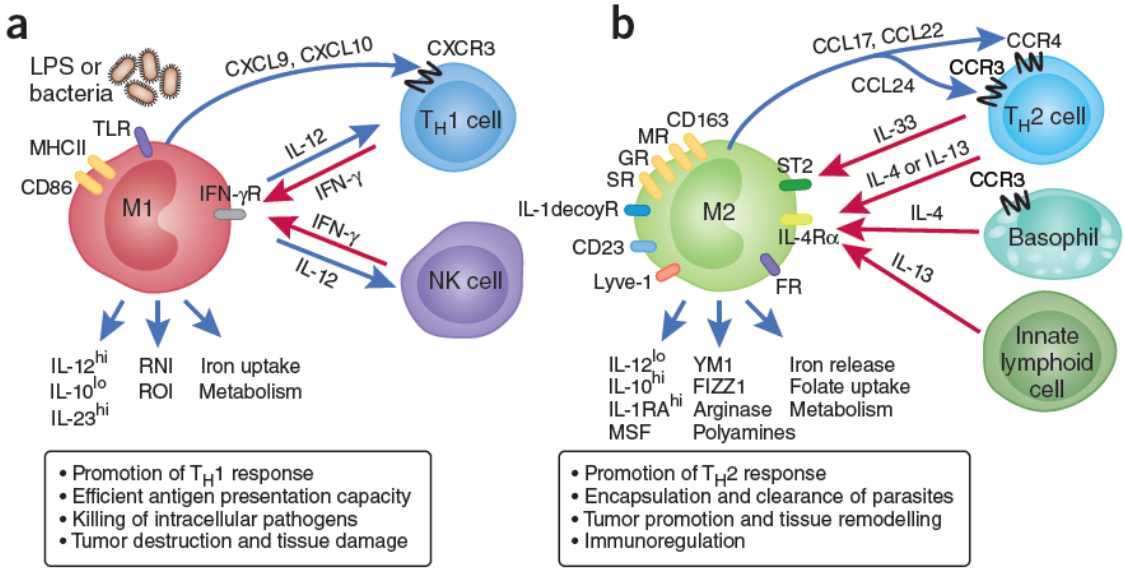


**Figure 4. Myeloid cell plasticity - modified from (Biswas and Mantovani, 2010)**

Macrophage activation and polarization by lymphoid cells. 1a. M1 polarized macrophages and their crosstalk with $T_H1$ cells and NK cells – M1 macrophages are characterized by a high expression of pro-inflammatory cytokines (IL.12, IL-13), high expression of reactive nitrogen- and reactive oxygen intermediates and low expression of IL-10. They are involved in the defense against bacterial cells, viruses and in anti-tumor immunity. 1b. M2 polarized macrophages driven by $T_H2$ cells, basophils and innate lymphoid cells through their secretion of IL-4, IL-33 and IL-13 – M2 macrophages are characterized by the up-regulation of certain marker genes (e.g. YM12, FIZZ1 and Arg1), they express high levels of IL-10 and low levels of IL-12 and are involved in the clearance of parasites, tumor promotion, tissue remodelling and immunoregulation.

### 1.4.3 Macrophage plasticity in cancer

Depending on the expression of different surface markers, marker genes, cytokines and chemokines, macrophages are polarized towards a particular phenotype, with many different stages possible in between the two extreme polarization states M1 and M2. Macrophages can also be polarized towards an M2-like phenotype, which is the case during

the progression of many types of disease including cancer. The M2-like phenotype shares some, but not all properties with IL-4 or IL-13 activated macrophages (see Figure 5) (Biswas and Mantovani, 2010; Mantovani et al., 2004). Various stimuli, containing antibody immune complexes together with LPS or Interleukin-1 (IL-1), glucocorticoids, transforming growth factor-ß (TGF-ß) and IL-10 give rise to M2-like macrophages which share some, but not all key features of alternatively activated M2 macrophages.

Monocytes including macrophages usually get recruited to the site of cancer related inflammation, where M1 macrophages can elicit anti-tumor immune response as well as tumor tissue disruption and contribute to T-cell mediated elimination and equilibrium phase during tumor progression (Mantovani et al., 2002).

A shift in monocyte-macrophage phenotypes has been previously observed during the progression of several diseases, including sepsis, obesity and most importantly cancer (Biswas and Mantovani, 2010). In the case of cancer, it has been shown that macrophages can contribute to tumor progression by their phenotypical conversion from the M1 pro-inflammatory state to the M2 immuno-tolerating state. Tumor associated macrophages (TAMs) are typically found in the close proximity to tumor masses and generally exhibit an M2-like phenotype characterized by low tumoricidal activity, the promotion of angiogenesis and tissue repair, high expression of IL-10 as well as a low expression of IL-12.

Another myeloid cell type typically found in the microenvironment of the majority of tumors are myeloid-derived suppressor cells (MDSCs). MDSCs are characterized by the expression of Gr1 and CD11b and represent myeloid precursor cells that expand during the course of various disease, including cancer, inflammation and infection. Through their ability to regulate T-cell functions they suppress adaptive immune responses and are implicated in tumor promotion (Gabrilovich and Nagaraj, 2009).

Myeloid derived suppressor cells are linked to tumor-associated macrophages and may be their precursors (Mosser and Edwards, 2008).

Tumor-associated macrophages generally exhibit an M2-like polarization and have been shown to have an immunosuppressive effect by their interaction with regulatory T-cells. $T_{reg}$ derived IL-10 has been shown to be involved in the suppression of inflammatory cytokines, by the activation of STAT3 which results in the up-regulation of SOCS3 which is an inhibitor of cytokine pathways, hence skewing macrophages towards an M2 polarization (Biswas and Mantovani, 2010).

Extracellular matrix components, IL-10, CSF-1 and various chemokines (e.g. CCL2, CCL18, CCL17, CXCL4) produced by tumor cells, have the potential of converting macrophages into an M2-like cancer promoting state (Mantovani et al., 2008a).

The PI3K/PTEN pathway plays an important role in this macrophage fate decision process as PTEN-deficiency in macrophages leads to a polarization towards the M2 phenotype. Macrophages and related cell types such as myeloid-derived suppressor cells, isolated from mouse and human tumors, generally exhibit an M2-like phenotype, characteristical for tumor associated inflammation (Biswas et al., 2008; Mantovani et al., 2002).

Myelomonocytic cells influence nearly all states of carcinogenesis and tumor progression, by promoting angiogenesis and lymphangiogenesis, by the suppression of adaptive immunity, by contributing to genetic alterations and instability, by promoting invasion and metastasis and many more. Tumor cells in turn, influence macrophages by the secretion of different chemokines and cytokines which promote M2-like polarization (such as CCL2, TGF-ß, IL-10, TNF, etc.) and by escaping phagocytosis (Biswas and Mantovani, 2010).

In a model for spontaneous mammary carcinoma driven by polyoma virus oncoprotein PyMT, it has not only been shown that the $TH_2$ derived cytokines IL-4 and IL-13 induce M2 polarization of tumor associated macrophages (TAMs), but also that blockage of IL-4 or the IL-4 receptor IL-4R α respectively diminishes lung metastasis and lowers the expression of M2 genes while increasing the expression of M1 genes (DeNardo et al., 2009).

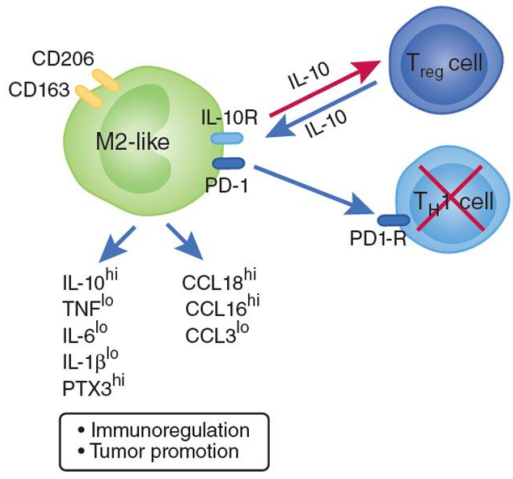


**Figure 5. M2-like macrophage phenotype - modified from (Biswas and Mantovani, 2010)**

Macrophages polarized in a M2-like state, share some but not all key features of M2 polarized macrophages. They express high levels of IL-10 and low levels of pro-inflammatory cytokines such as TNF and IL-6.

# 2. Aim of the study

As signaling via PI3K has many downstream effects including cell survival, promotion of cell proliferation, increase of glycolytic flux, inhibition of apoptosis and many more, the alteration of this pathway via the knockout of certain key players has become very intriguing. During the last few years, studies have shown that the PI3K pathway plays an important role in the regulation of inflammatory responses of macrophages, hypothesizing that active PI3K has an anti-inflammatory role in macrophages. This is based on the fact that the PI3K/PTEN pathway plays an important role in the fate decision process of macrophages and myeloid PTEN-deficiency leads to a shift in macrophage polarization states towards the alternatively activated M2 phenotype.

We therefore subjected myeloid PTEN knockout mice to a model of colitis-associated colon cancer, suggesting that conditional myeloid PTEN-deficiency, which results in an elevated activation of the PI3K pathway, leads to an enhanced suppression of pro-inflammatory, anti-tumor immune responses during the development of colitis-associated colon cancer. Based on this, we suggest that the reduction of immune-reactivity against tumor cells would lead to enhanced tumor growth.

The main focus of this study relates to the role of the PI3K/PTEN pathway in macrophages during inflammation driven colon cancer development, utilizing mice harbouring a PTEN knockout in all cells with an active lysozyme M (LysM) promoter which mainly affects phagocytic cells, including macrophages.

By analyzing these mice and different cell population taken from these animals after induction of colitis-associated colon cancer, we hope to increase our understanding of the role of the PI3K/PTEN pathway in myeloid cells, on the immune system during inflammation driven cancer development.

# 3. Materials and Methods

## 3.1 Mice

The knockout mice used for our experiments were all generated using the cre-lox recombination system which uses the enzyme cre-recombinase, isolated from the P1 bacteriophage (see Figure 6). By targeting a specific DNA sequence (in our case PTEN) by flanking it between two distant cre recognition sites, i.e. loxP sites, the desired sequence can be excised by the cre recombinase, which catalyzes site specific recombination via a crossover between the two loxP sites. DNA sequences flanked by loxP sites are termed as "floxed" and are spliced out by cre mediated recombination. Control of cre expression can be mediated by the use of an inducible system or by the utilization of an cell-type or tissue specific promoter. In our studies we used LysM cre knockout mice, indicating that the expression of the cre recombinase is dependent on the activity of the LysM promoter, assuring that PTEN is only excised in cells with an active LysM promoter.

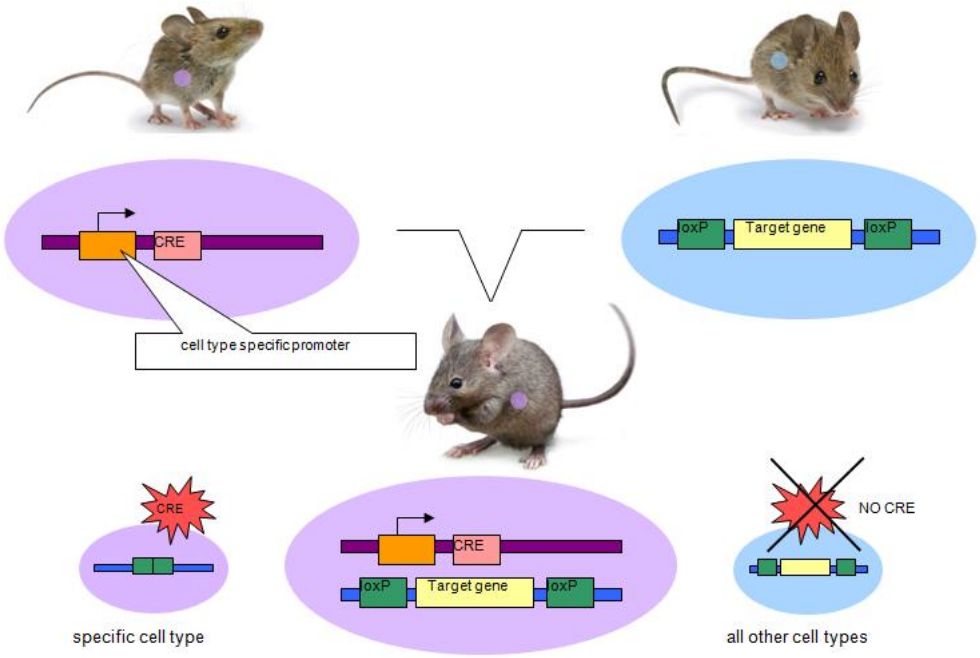


**Figure 6. The cre-lox system**

In order to obtain mice with a tissue or cell-type specific knockout, PTEN floxed/floxed mice where crossed to transgenic mice harbouring the cre recombinase behind a cell-type specific promoter.

All mice used in our experiments were bred and housed in a specific pathogen-free facility of the Medical University of Vienna with a 12-h/12-h day/night cycle and constant temperature.

Floxed PTEN mice were generously provided by Tak W. Mak (University of Toronto, Toronto, Canada) (Suzuki et al., 2001). LysM cre recombinase transgenic mice which were first described by Clausen et al (Clausen et al., 1999) and were kindly gifted from Randall Johnson (UCSD, La Jolla, CA, USA) (Peyssonnaux et al., 2005). Intercrossed mice were then backcrossed to a C57BL/6J background for at least eight generations.

For our experiments littermate-controlled experiments using mice of both sexes were performed with 8- to 12-week-old wild type (WT), floxed PTEN $cre^+$ and $cre^-$ mice. All in vivo experiments were performed according to institutional guidelines for animal experimentation, an ethical approval was obtained by the Federal Ministry for Science and Research, Vienna, Austria. (BMWF-66.009/0055-II/3b/2014). 3-4 weeks after their birth, mice were ear marked and their genotype was determined using PCR.

### 3.1.1 Ear Notching system

Via different ear punches mice are marked approximately 3-4 weeks after their birth, in order to distinguish individual mice from each other. The tissue particles produced by the ear punches are later on used for tissue lysis. The according numbers of the used Notching system can be seen in Figure 7.

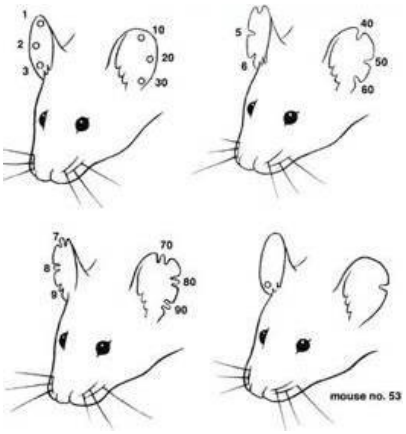


**Figure 7. Ear Notching System (modified from bu.edu – Boston university official homepage)**
Marks on the animal's right ear indicate units/ones: 1, 2, 3, etc.
Marks on the animal's left ear denote tens: 10, 20, 30, etc.
The sample mouse in the right corner was given the number 53.

## 3.2 Genotyping

### 3.2.1 Murine tissue lysis

**Materials**

Lysis Buffer (1M Tris HCl pH 8.0, 500mM EDTA pH 8.0, 10% SDS, 5M NaCl in 500 ml dH2O)
Proteinase K (2ng/ml, Roche Diagnostics, Germany))
Ear Punch (Fisher Scientific, USA)

**Methods**

The tissue pieces resulting from ear punching the mice are subsequently used for genotyping. 95µl of lysis buffer and 5µl of Proteinase K (2ng/ml) are therefore mixed and incubated with each sample for 3h on a thermoblock at 55°C, shaking with 600rpm. After 3h, the heat is turned up to 95°C for 5 minutes in order to stop the reaction. The reaction is then diluted with 1ml of ddH2O and samples are stored at 4°C and used for PCR reaction.

### 3.2.2 Polymerase chain reaction (PCR)

**Materials**

5x GoTaqR® Flexi Buffer (Promega)
GoTaqR® Flexi DNA Polymerase (Promega)
Magnesium Chloride Solution, 25 mM (Promega)
dNTP mix, 25 mM (Thermoscientific)
Eppendorf twin.tec PCR 96 well plate,
skirted Thermo Scientific Adhesive PCR Sealing Foil Sheets
Eppendorf Mastercycler

**Methods**

In order to determine the genotypes of the mice used for our experiments, PCR is performed using primers to amplify the cre gene and floxed PTEN alleles. For each sample, 5µl GOTaq

Flexi Buffer, 12,875µl $dH_2O$, 2,5µl dNTPs, 2,5µl MgCl, 1µl Primer mix and 0,125µl GOTaq DNA Polymerase are mixed and pipettet into a 96 well plate, were 2µl of sample are added. Primers used for the amplification of floxed PTEN alleles and the cre gene, can be obtained from Table 1. The used PCR program is shown in Table 2.

| Step | Temperature | Time | Number of Cycles |
|---|---|---|---|
| **Initial Denaturation** | 94°C | 5 minutes | 1 |
| **Denaturation** | 94°C | 30 seconds | 40 |
| **Annealing** | 57°C | 30 seconds | |
| **Extension** | 72°C | 45 seconds | |
| **Final Extension** | 72°C | 2 minutes | 1 |
| **Cool Down** | 4°C | indefinite | 1 |

**Table 1. PCR program used for amplification of PTEN and cre genes**

| Gene | Forward Sequence (5' → 3') | Reverse Sequence (3' →5') |
|---|---|---|
| **PTEN** | CTC CTC TAC TCC ATT CTT CCC | ACT CCC ACC AAT GAA CAA AC |
| **Cre** | TCG CGA TTA TCT TCT ATA TCT TCA | GCT CGA CCA GTT TAG TTA CCC |

**Table 2. Primersequences used for amplification of PTEN and cre genes**

### 3.2.3 Agarose Gel Electrophoresis

**Materials**

50x TAE Buffer (242 g Tris base, 71.1 ml Glacial acetic acid, 100 ml 0.5 M EDTA [pH 8.0] added up to 1000 ml with dH2O)

Agarose (Biozym LE Agarose)

peqGREEN (peqlab)

Gene Ruler™ 1 kb DNA Ladder (Fermentas)

**Methods**

To visualize PCR products, 10µl of each PCR reaction sample is loaded onto a 2% Agarose gel. The gel is prepared by filling up 5g of agarose with 250ml TAE buffer and heating up the

mixture in the microwave until the agarose is completely dissolved. After giving the liquid gel a chance to cool down for a few minutes, 20µl of peqGREEN is added and the gel is casted into the gel tray with appropriate combs. 8µl oft the 1kb DNA Ladder (see Figure 8.) are loaded onto the gel in order to identify the sizes of our specific PCR products afterwards. The gel then runs for 90 minutes at 120V. Finally pictures are taken with a UV-Gel documentation system (peqlab) and bands were analyzed according to their molecular weight in order to obtain genotypes.

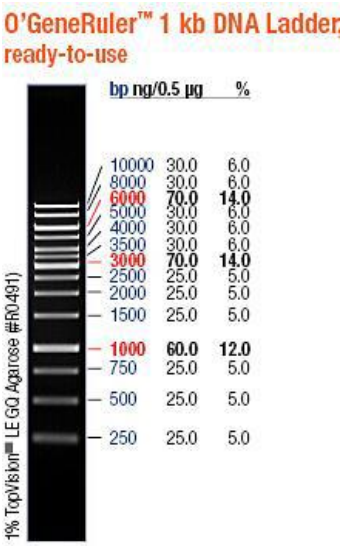


**Figure 8. 1 kb DNA Ladder ready-to use**

(modified from thermoscientificbio.com) Ladder used for gelelectrophoresis

## 3.3 RNA Analysis

### 3.3.1 RNA Isolation

**Materials**

peqGOLD TriFast (peqlab)

Isopropanol water free (Fischer Scientific, USA)

Chloroform (Carl Roth GmbH, Germany)

UltraPure DEPC-treated Water (Invitrogen Corporation, CA, USA)

RNase free water (Qiagen)

**Methods**

500 µl of TriFast reagent are added to approximately 20-30 mg of tissue sample and homogenized using a tissue homogenizer (precellys – bertin technologies). After homogenization at 5000 rpm for 20 seconds, samples are incubated at room temperature (RT) for 5 minutes (min), before 250 µl chloroform per 500 µl of TriFast agent are added. The mixture is shaken vigorously by hand for 15 seconds (sec) and again incubated at RT for 3 min, before samples are centrifuged at 12 000 x g for 15 min at 4°C. After removing the aqueous phase and placing it into a fresh tube, we continue with RNA precipitation. Therefore 500 µl of 100 % Isopropanol per 1 ml of TriFast reagent are added to the samples and the mixture is incubated at RT for 10 min. After the incubation step samples are centrifuged at 12 000 x g for 10 min at 4°C and the supernatant is removed. The pellet containing the RNA is washed with 1 ml of 75 % ethanol (EtOH) per 1 ml of TriFast reagent used in initial homogenization. After briefly vortexing the samples, they are centrifuged @ 7500 x g for 5 min at 4°C and supernatant is discarded. After repeating the washing step, the RNA pellet is given time to dry until all EtOH is evaporated. Finally the pellet is resuspended in an appropriate amount of RNase-free water and incubated at 55°C for 15 min. To determine RNA concentrations and purity of our samples we use a nanodrop (Nanodrop 2000 Spectrophotometer – peqlab) Once the RNA pellet is dissolved in RNase-free water, it can be stored at -70°C.

The RNA Isolation method described above was used for many of our experiments, however we did also work with an RNA isolation kit (RNeasy® Mini Kit – Qiagen) in order to extract RNA from our samples. When working with the kit, we used the included reagents only and followed the supplied protocol for tissue homogenization, RNA isolation and precipitation.

### 3.3.2 Reverse Transcription

**Materials**

High-Capacity cDNA Reverse transcription Kits (Applied Biosystems, USA)

UltraPure DEPC-treated Water (Invitrogen Corporation, USA)

Eppendorf Mastercycler

**Methods**

In order to perform the reverse transcription, we prepare a master mix which includes 2 µl RT buffer, 0,8 µl dNTP Mix (100 nM), 2,0 µl RT random primers, 1 µl RNase Inhibitor and 3,2 µl nuclease-free water per sample. 10 µl of each sample (diluted to transcribe 1 µg of RNA) is pipette into the reaction tubes and 10 µl master mix is added per sample.

The program used on the eppendorf mastercycler can be obtained from table 3. After the program is finished and samples have cooled down, cDNA can be stored at -20°C or used for qPCR respectively.

| Step | Temperature | Time |
|---|---|---|
| **1** | 25°C | 10 min |
| **2** | 37°C | 120 min |
| **3** | 85°C | 5 min |
| **4** | 4°C | ∞ |

**Table 3. PCR program used for high capacity reverse transcription PCR**

### 3.3.3 Quantitative real-time PCR

**Materials**

Fast SYBR® Green Master Mix (Applied Biosystems, Life Technologies Corporation, USA)

UltraPure DEPC-treated Water (Invitrogen Corporation, USA)

Multiply PCR-Plates 96 well (Sarstedt, Nümbrecht, Germany)

Adhesive PCR foil (Sarstedt, Nümbrecht, Germany)

StepOne Real-Time PCR System (Applied Biosystems)

**Methods**

The preparation of the master mix and the subsequent pipetting of the samples and the master mix into the PCR plate is performed on ice and under protection from light.

The master mix is prepared by mixing 5,25 µl of DEPC water, with 7,5 µl Fast SYBR® Green Master Mix and 0,375 µl of each of the according primers. After pipetting 1,5 µl of each cDNA sample into the plate, 13,5 µl of master mix are added to each sample. Hypoxanthine phosphoribosyltransferase (HPRT) is used as a reference gene. The primers used for qPCRs can be obtained from table 4. The qPCR was performed using the StepONE Real-Time PCR System (Applied Biosystems).

| Gene | Forward Sequence (5' → 3') | Reverse Sequence (3' →5') |
|---|---|---|
| **GAPDH** | GGTCGTATTGGGCGCCTGGTCACC | CACACCCATGACGAACATGGGGGC |
| **HPRT** | CGCAGTCCCAGCGTCGTG | CCATCTCCTTCATGACATCTCGAG |
| **PTEN** | ACACCGCCAAATTTAACTGC | TACACCAGTCCGTCCCTTTC |
| **Arg 1** | GTGAAGAACCCACGGTCTGT | CTGGTTGTCAGGGGAGTGTT |
| **Ym1** | TTTCTCCAGTGTAGCCATCCTT | TCTGGGTACAAGATCCCTGAA |
| **Fizz 1** | CTGGATTGGCAAGAAGTTCC | CCCTTCTCATCTGCATCTCC |
| **IL-10** | AGCTGAAGACCCTCAGGATG | TGGCCTTGTAGACACCTTGG |
| **IL-23** | ATGCTGGATTGCAGAGCAGT | ACGGGGCACATTATTTTTAG |
| **IL-6** | TGCAAGTGCATCAT GTTGTTC | CCACGGCCT TCCCTACTTCA |
| **TNFα** | CCACCACGCTCTTCTGTCTAC | AGGGTCTGGGCCATAGAACT |

**Table 4. Primersequences used for cDNA amplification during quantitative real-time PCR**

## 3.4 Induction of colitis-associated colon cancer with AOM/DSS

### Materials

Disposable Insulin Needle (27G x ½", Braun)

Syringe (Omnifix®)

Azoxymethan (AOM, Sigma Aldrich)

Dextran Sulfate Sodium (DSS, Sigma Aldrich)

### Methods

Mice are injected with 5 µl (=12.5 mg/kg bodyweight) of the carcinogen Azoxymethan (AOM) per g of bodyweight into the intra peritoneal at day zero. At day 6 the first cycle of dextran sodium sulfate (DSS) starts, with the chemical being dissolved into the mice's drinking water. DSS treatment lasts for six days each and is interspersed by three cycles of pure drinking water for 15 days each. After 3 cycles of DSS are completed, mice are kept on drinking water until the experiment comes to an end between 80 to 90 days after the administration of AOM. The amount of DSS dissolved into the ice drinking water per cycle as well as the treatment periods can be obtained from Table 5.

| | Monday | Tuesday | Wednesday | Thursday | Friday | Saturday | Sunday |
|---|---|---|---|---|---|---|---|
| Week1 | | | | AOM | | | |
| Week2 | | | | | 2,5% DSS | | |
| Week3 | | | | | | | |
| Week4 | | | | | | | |
| Week5 | | | | | 2,5% DSS | | |
| Week6 | | | | | | | |
| Week7 | | | | | | | |
| Week8 | | | | | 2,0% DSS | | |
| Week9 | | | | | | | |
| Week10 | | | | | | | |
| Week11 | | | | | | | |
| Week12 | | | | | | | |
| Week13 | sacrifice | | | | | | |

**Table 5. Experimental setup for the induction of colitis-associated colon cancer using AOM and DSS**

## 3.5 Isolation of organ samples

**Materials**

Ketaminol® (Intervet International GmbH, Germany)

Xylasol® (Dr. E. Gräub AG, Bern, CH)

Phosphate Buffered Formaldehyde (Roti® Histofix 4%, Carl Roth GmbH, Germany)

Cell Medium: RPMI + 10 % Fetal Calf Serum (FCS) + L- glutamine + PenStrep (Penicillin and Streptomycin)

Disposable Insulin Needle (27G x ½", Braun)

Syringe (Omnifix®)

**Methods**

After weighing the mice, mice are sedated via an intraperitoneal injection with a mixture of Ketaminol and Xylasol (Hellabrunner mixture: 3. 5 mg/kg Ketaminol® and 50 mg/kg Xylasol®) according to their bodyweight (1 µl Ketaminol/Xylasol per 1 µg bodyweight). Afterwards mice are opened using sterile surgical instruments, skin is removed and organs are put aside to uncover the vena cava. A blood sample is then taken using a 27G syringe and blood is centrifuged at 5000 rpm for 5 min, to obtain serum which is transferred into a new tube and stored at -20°C for further analysis (e.g. ELISA). The spleen, the colon and the mesenteric lymph node are isolated and stored in PBS (phosphate buffered saline) for further progression. Depending on the experiment, organs are treated appropriately. If organs are used for histological analysis, they are placed in a histocassette and stored in a Phosphate Buffered Formaldehyde bath (Roti® Histofix 4%, Carl Roth GmbH, Germany) over night. In case of the colon, the organ is first flushed with PBS and then with 4% PFA and arranged in a colonic swiss role (see Figure 9) before it is placed in the histocassette. The next day the Formaldehyde solution is discarded and cassettes are stored in 70% EtOH until samples are taken to the general hospital of Vienna (AKH Wien – Allgemeines Krankenhaus Wien) for the dehydration and paraffinization process (see 3.9).

In case organ samples are used for subsequent cell isolation, a small aliquot is taken from each organ to get snap frozen in liquid nitrogen for further analysis (e.g. homogenization

followed by RNA isolation, ELISA or westernblot), the rest of the organ is stored in RPMI full medium on ice to proceed with cell isolation.

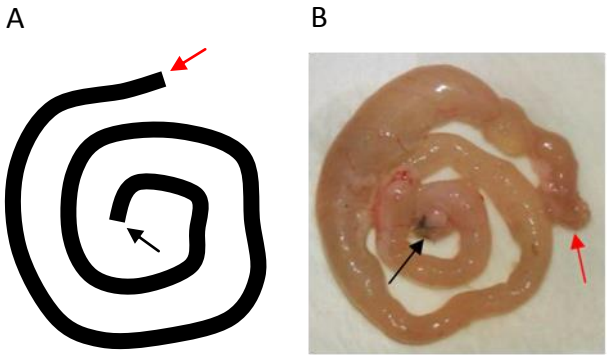


**Figure 9. colonic swiss role**

For histological analysis, the colon is arranged into a swiss role. A. Schematic view of the colonic swiss role, black arrow indicated the anus, red arrow points to the part of the colon where it was cut underneath the cecum. B. Example of a colonic swiss role before organ is inserted into histocasette.

## 3.6 Cell isolation from murine spleen and mesenteric lymph node

**Materials**

Cell Medium: RPMI + 10 % Fetal Calf Serum (FCS) + L- glutamine + PenStrep (Penicillin and Streptomycin)

Collagenase D solution (10 mg/ml PBS) (incl. 100 U/ml Hyaluronidase (100x= 10.000 U/ml) and 10 µg/ml DNAse I (100x = 1 mg/ml))

CD11b MicroBeads catalogue-no 130-049-601 (MACS® Miltenyi Biotech)

CD11c MicroBeads catalogue-no 130-052-001 (MACS® Miltenyi Biotech)

CD4 MicroBeads catalogue-no 130-049-201 (MACS® Miltenyi Biotech)

Miltenyi MS or LS Columns (MACS® Miltenyi Biotech)

autoMACS Running Buffer – MACS Separation Buffer catalogue-no 130-091-221 (MACS® Miltenyi Biotech)

**Methods**

### 3.6.1 Isolation of splenocytes

Isolated spleens are placed into a 12-well plate filled with 1 ml of collagenase D solution and injected with 1 ml of collagenase D solution by using a 27G syringe. Tissue is then cut into smaller pieces using sterile scissors. A further ml of collagenase D solution is added into each well before the plate is incubated at 37°C for 30 minutes. After the incubation time, the digestion mixture is resuspended using a serological pipette and remaining tissue is smashed through a 70 µm cell strainer and cells are transferred into a 15 ml falcon tube. Cells are centrifuged at 300 x g for 7 min at 4°C and washed 2 times with 5 ml PBS. In order to eliminate erythrocytes, an erylysis is performed, resuspending each cell pellet in 1 ml erylysis buffer followed by an incubation step of 5 minutes at room temperature (RT). PBS is added to stop the reaction and samples are centrifuged at 300 x g for 7 min at 4°C. After resuspension of each pellet in PBS, an aliquot of the cell suspension is taken for cell count analysis.

### 3.6.2 Sample preparation for magnetic isolation of $CD11b^+/CD11c^+$ and $CD4^+$ cells

Labelling of $CD11b^+$ cells

$10^7$ cells are resuspended in 90 µl of MACS buffer and 10 µl of CD11b Micro beads per $10^7$ cells are added. The mixture is then incubated at 4°C for 10 minutes. Afterwards cells are washed by the addition of 1-2 ml buffer per $10^7$ cells and samples are centrifuged at 300 x g for 10 min at 4°C. Finally up to $10^8$ cells are resuspended in 500 µl MACS buffer before we proceed with the magnetic isolation.

Labelling of $CD11c^+$ cells

Up to $10^8$ cells are resuspended in 400 µl of MACS buffer and 10 µl of CD11c Microbeads per $10^7$ cells are added. The mixture is then incubated at 4°C for 10 minutes. Afterwards cells are washed by the addition of 1-2 ml buffer per $10^7$ cells and samples are centrifuged at 300 x g for 10 min at 4°C. Finally up to $10^8$ cells are resuspended in 500 µl MACS buffer before we proceed with the magnetic isolation.

Labelling of $CD4^+$ cells

Up to $10^7$ cells are resuspended in 40 µl of MACS buffer and 10 µl of Biotin-Antibody cocktail per $10^7$ cells are added. The mixture is then incubated at 4°C for 5 minutes. Afterwards 30 µl of buffer are added per $10^7$ cells and 20 µl of Anti-Biotin microbeads cocktail is added per $10^7$ cells. The mixture is then incubated at 4°C for 10 min. Afterwards buffer is added to the cells to fill up to a minimum of 500 µl before we proceed with the magnetic isolation.

### 3.6.3 Magnetic isolation of $CD11b^+/CD11c^+$ and $CD4^+$ cells

Isolation of $CD11b^+$ and $CD11c^+$ cells

The column is first placed into the magnetic field and rinsed with MACS buffer (MS: 500 µl, LS: 3 ml), before the cell suspension is applied onto the column. The column is washed three times with MACS buffer (MS: 3x 500 µl, LS: 3x 3 ml) and flow-through is collected. Finally the column is removed from the separator and buffer is applied onto the column (MS: 1 ml, LS: 5 ml) and

magnetically labelled cells are flushed out of the column via the means of a plunger. An aliquot of approximately 2 x $10^6$ cells is taken for cell surface marker analysis (FACS) and a small aliquot is taken for cell count analysis.

Isolation of $CD4^+$ cells

The isolation procedure for $CD4^+$ cells is identical to the isolation of $CD11b^+$ and $CD11c^+$ cells, except that in this case, magnetically labelled $CD4^+$ cells are negatively selected and therefore obtained from the collected flow-through.

### 3.6.4 Restimulation of splenocytes with anti-CD3$^{epsilon}$

In order to specifically stimulate and expand T cell populations, cells are treated with the anti-CD3 ligand. For this purpose we used soluble anti-CD3 as well as plate bound anti-CD3. For the plate bound ligand, cell culture plates are coated with 5 µg/ml anti-CD3 in PBS and incubated overnight at 4°C. Plates are washed with PBS the next day and $10^7$ cells/ml which were resuspended in RPMI full beforehand are added to the plates. When working with soluble anti-CD3, 100 ng/ml anti-CD3 were added to $10^7$ cells/ml directly. In both cases supernatants for ELISA are taken on day1 and day 3, and the cells are resuspended in Trios at day 3 for further RNA analysis (see 3.3).

## 3.7 Enzyme Linked Immunosorbent Assay (ELISA)

**Materials**

0.05% PBS-T (1 x PBS mixed with PlusOne Tween-20 (GE Healthcare, Bio-Science AB)

Blocking solution (1 % BSA in 1 x PBS)

TMB 2-Component Micro well Peroxidise Substrate Kit (VWR International, Austria)

2 N $H_2SO_4$

F8 Maxisorb Loose Nunc-Immuno Module (Thermo Scientific-Nunc A/S, Denmark)

Bio-Tek EL808 Ultra Microplate Reader (Bio-Tek Instruments, USA)

Streptavidin-HRP (R&D Systems, USA)

Mouse Interleukin-10 (IL-10), DuoSet® ELISA kits (R&D Systems, Minneapolis, USA)

Mouse Interleukin-17A (IL-17A), ELISA Ready-Set-Go!® Kit ( 13-7177, eBioscience Inc., USA)

Mouse Interferon-gamma (INF-γ), Ready-SET-Go!® Kit (eBioscience Inc., USA)

Mouse Interleukin-6 (IL-6), DuoSet® ELISA kits (R&D Systems, Minneapolis, USA)

Mouse tumor necrosis factor alpha (TNFα), DuoSet® ELISA kits (R&D Systems, Minneapolis, USA)

**Methods**

Supernatant levels of secreted cytokines were determined using commercially available antibodies directed against the according cytokines.

To perform ELISA, we coat 96 well plates with the coating antibodies directed against the desired cytokine. Antibodies are diluted in PBS according to the manufacturers' protocol and plates are incubated with the coating antibody overnight at 4°C on a shaker. Plates are washed three times with 0.05% PBS-T the following day and wells are then incubated with the blocking solution for at least 2 hours at room temperature. After the incubation step, plates are washed again three times with 0.05% PBS-T and samples are loaded onto the plates in an appropriate dilution and plates are incubated overnight at 4°C slowly shaking. At day three samples are again washed in the same manner before the detection antibody is pipetted into the wells, diluted in 1% PBS-BSA according to the manufacturers' protocol and plates are incubated for 2-3 hours at room temperature. Afterwards plates are washed with 0.05% PBS-T four times and Streptavidin diluted in 1% PBS-BSA (1:200) is pipette into the

plates and plates are incubated at room temperature, protected from light for at least 20 minutes shaking. Finally samples are washed six times with 0.05% PBS-T and the TMB-Substrate solution (1:1) is used to develop the plates (70 µl per well). Samples are incubated with TMB substrate for five to ten minutes according to the degree of staining before the enzymatic reaction is stopped by pipetting 35 µl of 2 N H2SO4 into each well. Finally concentrations of the cytokines are measured via the intensity of the colour produced during the TMB reaction. For the measurement we use the Bio-Tek EL808 Ultra Microplate Reader (Bio-Tek Instruments, USA) at 450 nm and 540 nm.

## 3.8 Immunoblotting

**Materials**

Solution A (30 g Acrylamid, 0,8 g Methylenbisacrylamid in 100 ml $dH_2O$)

Solution B (18,2 g Tris, 0,4 g SDS in 100 ml $dH_2O$; pH: 8,8)

Solution C (6,06 g Tris, 0,4 g SDS in 100 ml $dH_2O$; pH: 6,8)

APS (10 g Ammoniumpersulfat in 100 ml $dH_2O$)

TEMED (Roth)

Laemmli buffer (12,5 ml solution C, 5 ml Mercaptoethanol, 11,5 ml 87% Glycerol, 2g SDS, 5 mg Bromphenol Blue in 50 ml $dH_2O$)

Running Buffer (4x: 12 g Tris, 57,6 g Glycin, 4 g SDS in 1000 ml $dH_2O$)

Blotting Buffer (250 ml 4x Running Buffer, 200 ml Methanol in 1000 ml $dH_2O$)

0.5% PBS-T (1 x PBS mixed with PlusOne Tween-20 (GE Healthcare, Bio-Science AB)

Blocking solution (5 % milk powder in 0.5% PBS-T)

polyvinylidene difluoride transfer membrane (Millipore, Bedford, MA, USA)

Trans-Blot® Turbo™ Transfer System

chicken anti–Arginase 1 antibody (kindly provided by Dr. Morris)

rabbit antibody anti-PTEN (Cell Signalling Technology)

rabbit antibody anti-Actin (Sigma)

anti-chicken peroxidase-conjugated secondary antibody (Cell Signalling Technology)

anti-rabbit peroxidase-conjugated secondary antibody (Cell Signalling Technology)

SuperSignal West Femto (Pierce)

FluorChem HD2 chemiluminescence imager (Alpha Innotech)

**Methods**

Samples are lysed in Laemmli buffer and separated on a 12% denaturing polyacrylamide gel (1,65 ml Solution A, 0,8 ml $dH_2O$, 2,5 ml Solution B, 10 µl TEMED, 20 µl APS). After separation (constant 40 mA per gel), protein bands are blotted onto a polyvinylidene difluoride transfer membrane using the Trans-Blot® Turbo™ Transfer System. After the transfer, the membrane is incubated in a bath of blocking solution for at least 20 minutes at room temperature on a shaker. After blocking, membranes can be incubated with the primary antibodies, which were diluted in 5% milk powder in 0.5% PBS-T according to the manufacturers' manual. Membranes are incubated with the primary antibody over night at 4°C on a shaker. Membranes are washed three times in 0.5% PBS-T the next day for 10 minutes each on a shaker, before they are incubated with the secondary antibody diluted in 5% milk powder in 0.5% PBS-T according to the manufacturers' manual, for at least two hours at room temperature on a shaker. Finally membranes are washed again for three times and protein bands are detected using the FluorChem HD2 chemiluminescence imager.

## 3.9 Immunohistochemistry

### 3.9.1 Tissue preparation

**Materials**

Roticlear (Roth)

Superfrost Plus Microscope Slides (VWR Vienna, Austria)

Coverslips (24 x 40cm Menzel and 24x 60cm Carl Roth GmbH, Germany)

Microtome (Shandon Finesse E+, Thermo scientific)

Leica EG1150 C cold plate Tissue Float Bath (GFL®)

Phosphate Buffered Formaldehyde (Roti® Histofix 4%, Carl Roth GmbH, Germany)

HistoStar (Thermo Fischer Scientific, USA)

**Methods**

According to 3.5 Isolation of organ samples, the colon was flushed with PBS and 4% PFA and arranged in a colonic swiss role before placed in the histocasette bathed in 4% PFA for 24 hours. The Formaldehyde solution is exchanged for 70% EtOH the next day and samples are stored in 70% EtOH until samples are taken to the general hospital of Vienna (AKH Wien – Allgemeines Krankenhaus Wien) for the dehydration and paraffinization process.

At the general hospital samples are removed from the cassettes and washed with 1x PBS. After they are incubated in 10% paraformaldehyd for two days at room temperature, the dehydration step begins by bathing samples in 75% EtOH over night, followed by a two hour incubation in 95% EtOH before samples are put into 100% EtOH over night at room temperature. The following day samples are incubated at 37°C in 100% EtOH for 30 minutes before they soak in 100% roticlear for 30 minutes at 37°C. After thirty minutes the temperature is raised to 60°C to incubate the samples for another 30 minutes. Next organs are put into bottle filled with a 1:1 paraffin wax/roticlear mixture for 24 hours at 60°C. Afterwards the bottle is opened at 60°C for 48 hours to give the solvents a chance to evaporate. Samples are then stored at 37°C until we pick them up to embed them in paraffin to proceed with further analysis.

Using a embedding machine (HistoStar, Thermo Fischer Scientific, USA), organs are embedded in paraffin. Once the paraffin is dried, histoblocks can be sliced into thin tissue sections via the use of a precision rotary microtome. Approximately 2 µm thick organ sections are produced and put in the tissue float bath to help the sections unravel before they are transferred onto the microscope slides and given a chance to dry.

### 3.9.2 Haematoxylin and Eosin Stain

**Materials**

Mounting Medium (Aquatex, Merck)

Eosin (0.5% in water, Carl Roth GmbH, Karlsruhe, Germany)

Xylene Substitute (Xylol Isomere, Lactan, 4436.2)

Mayer's Hemalaun (Merck, Calbiochem)

**Methods**

Before starting with the haematoxylin and eosin staining, slides have to be deparaffinised. In order to do so, slides are places at 60°C for 15 minutes and then incubated with Xylene for another 10 minutes. By putting the slides in 96% EtOH twice for two minutes flowed by 80% EtOH, 70% EtOH and $dH_2O$ once for one minute each, sections get rehydrated. The staining procedure begins by incubating each slide with haematoxylin solution for three minutes before the reaction is stopped with water and slides are incubated with eosin for two minutes before they get washed with $dH_2O$. In case the staining appears to strong, the pigmentation can be extenuated with 1% acid alcohol. Once slides are stained as desired, they are mounted and covered with cover slips.

## 3.10 Flow Cytometry

**Materials**

PC-Cy5.5 – GR-1 (BD pharma)

PE-Cy7 – CD11b (eBioscience)

APC – F4/80 (eBioscience)

FITC – Ly6G (eBioscience)

PE – CD103 (BD pharma)

APC-Cy7 – CD11c (BD pharma)

**Methods**

In order to prepare our samples for FACS analysis, $10^6$ cells of the respective organ were harvested and prepared per mouse and staining. First cells are centrifuged at 377 x g for 10 minutes at 4°C, supernatant is discarded and cells are resuspended in the remaining liquid by vortexing. Afterwards cells are resuspended in 800 µl PBS and again centrifuged at 377 x g for 10 minutes at 4°C. In order to stain our cells with different antibodies, a staining mix was prepared containing all antibodies diluted according to the manufacturers' protocol. Each sample is incubated with 50 µl of the staining mix for 20 minutes on ice, protected from light. After the incubation period, 800 µl of PBS are added to the mixture and cells are centrifuged for 10 minutes at 377 x g at 4°C, the supernatant is discarded and cells are resuspended in 200 µl of sheath fluid to continue with FACS analysis. Cell acquisition was performed on a flow cytometer (BD Science FACS Canto II) at the general hospital of Vienna and FlowJo software Version 10.0 was used for data analysis.

## 3.11 [3H]Thymidine proliferation assay

T cell proliferation was measured via the use of a [$^3$H]thymidine proliferation assay, in order to quantify T cells after in vitro stimulation. Cells were labelled via the incorporation of [$^3$H]thymidine (1 µCi/well) and incubated for 20 hours. After the incubation period, incorporation of [$^3$H]thymidine was measured in order to quantify cell proliferation. The assay was performed at the general hospital of Vienna (AKH – Allgemeines Krankenhaus Wien).

## 3.12 Preparation and cultivation of peritoneal macrophages

**Materials**

Thioglycollate (Sigma)

RPMI 1640 (Invitrogen)

ultrapure E. coli O111: B4 LPS (Invivogen)

wortmannin (Sigma)

N-hydroxy-L-arginine (Calbiochem)

recombinant mouse IL-4/IL-13 (R&D Systems)

**Methods**

In order to obtain peritoneal macrophages, mice were injected with 2 ml of 4% thioglycollate into the intraperitoneal before peritoneal lavage was performed three days later with RPMI medium. $10^6$ cells/ml were seeded in RPMI including 10% FCS, 1% penicillin-streptomycin-fungizone and 1% L-glutamine and cultured at 37°C over night. The next day in vitro stimulations were carried out by the addition of 100 ng/ml ultrapure *E.coli O111*: B4 LPS, 100 nM wortmannin, 10 or 200 mM N-hydroxy L-arginine or 5 ng/ml IL-4/IL-13. Cells were harvested 3, 8 and 24 hours after stimulation.

## 3.13 Preparation and cultivation of bone marrow–derived DCs

**Materials**

recombinant mouse GM-CSF (R&D Systems)

Cell Medium: RPMI + 10 % Fetal Calf Serum (FCS) + L- glutamine + PenStrep (Penicillin and Streptomycin)

**Methods**

Bone marrow cells were isolated from femurs and tibias and cultivated in RPMI medium containing 20 ng/ml GM-CSF at 37°C. After three and six days respectively, half of the medium is discarded and replaced with fresh media supplemented with GM-CSF in the same concentration used for primary cultivation. Dendritic cells were harvested at day 7 and used for further analysis.

## 3.14 Statistic

Statistical significance of data was evaluated by an unpaired two-tailed Student *t* test by the use of GraphPad Prism software (GraphPad Software, La Jolla, CA). Results are presented as the mean ± SD. P-values smaller than 0.05 are considered as statistically significant. P- values are illustrated as followed: * $p<0.05$, ** $p<0.01$, *** $p<0.001$.

# 4. Results

## 4.1 *Preliminary data*: PTEN loss leads to an up-regulation of IL-10 in macrophages

Previous experiments performed by our group, could show that the anti-inflammatory cytokine IL-10, is up-regulated in peritoneal macrophages isolated from PTEN$^{fl/fl}$ LysM cre+ mice, as compared to macrophages isolated from the peritoneal cavity of wild type littermate controls (Günzl et al., 2010). Isolated cells were cultured and restimulated with gram-negative LPS and quantitative real-time PCR was performed to quantify levels of IL-10 mRNA at the indicated time points after LPS stimulation of PTEN +/+ and PTEN -/- macrophages (see Figure 10A). Levels of IL-10 secreted into the supernatant of cultivated cells, were determined by ELISA analysis (see Figure 10B).

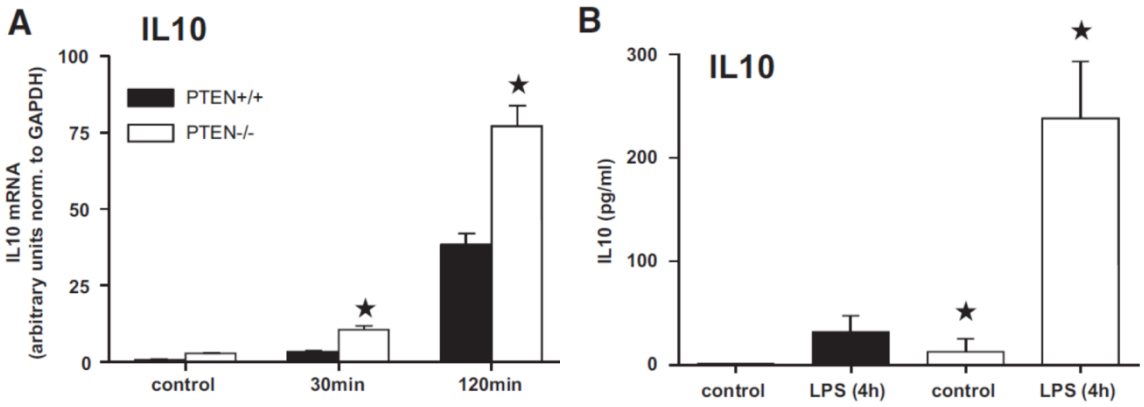


**Figure 10. IL-10 is up-regulated in PTEN-deficient macrophages**

A. Relative mRNA expression levels of IL-10 expressed by intraperitoneal macrophages isolated from PTEN +/+ and PTEN -/- mice at indicated time points after stimulation with gram-negative LPS. B. Cytokine levels of secreted IL-10 4h post LPS induction, measured by ELISA analysis. Statistical significance is indicated by *P < 0,05.

## 4.2 *Preliminary data*: The pro-inflammatory cytokines TNFα and IL-6 are down-regulated in PTEN-deficient macrophages

Preliminary data show that PTEN-deficiency in macrophages leads to a decrease in TNFα- and IL-6 mRNA levels. Furthermore, the amount of TNFα- and IL-6 protein secreted into the supernatant is enhanced in macrophages isolated from knockout animals when compared to cells obtained from littermate control mice (Günzl et al., 2010). Transcription of TNFα and IL-6 was quantified using semi-quantitative real-time RT-PCR 240 minutes upon stimulation of macrophages with heat-killed *A. Baumannii* (see Figure 11A). Levels of secreted TNFα and IL-6 were measured after stimulation of macrophages with different toll-like-receptor-ligands (see figure 11B). A decrease in TNFα and IL-6 mRNA levels was found in PTEN -/- macrophages, compared to PTEN +/+ macrophages after in vitro stimulation of cells with heat-killed *A. Baumannii*. Correspondingly cytokine levels of PTEN-deficient macrophages were decreased in comparison with wild type macrophages after stimulation.

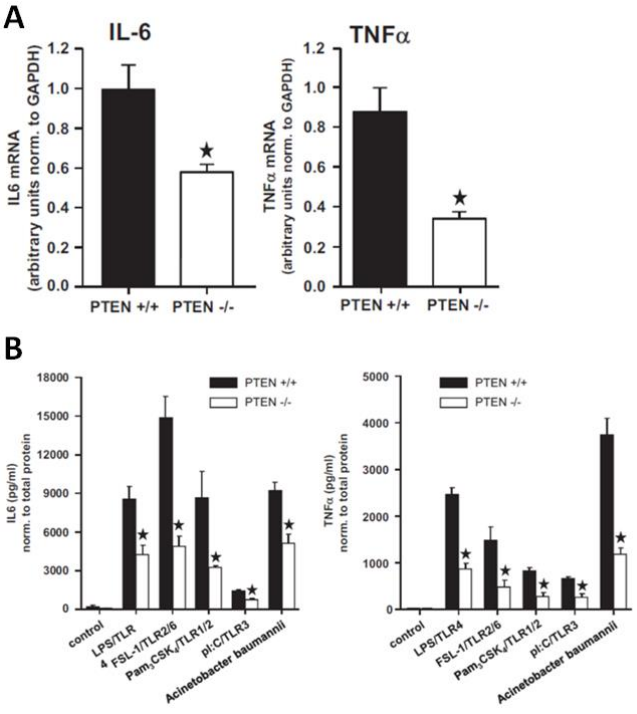


**Figure 11. PTEN-deficiency in macrophages leads to a down-regulation of TNFα and IL-6 mRNA and cytokine levels**

A. Peritoneal macrophages isolated from PTEN -/- mice show decreased mRNA levels of IL-6 and TNFα after stimulation with heat-killed *A. Baumannii.* B. Cytokine levels of secreted IL-6 as well as TNFα are reduced in PTEN -/- macrophages after stimulation with various toll-like-receptor-ligands (LPS, FSL-1, $Pam_3CSK_4$, pI:C9) and heat-killed *A. Baumannii*. Statistical significance is indicated by *P < 0.05.

## 4.3 *Preliminary data*: Arginase 1 is up-regulated in PTEN-deficient macrophages and bone marrow-derived dendritic cells

Preliminary experiments, show that PTEN-deficiency leads to a drastic change in Arginase 1 (Arg1) expression. PTEN-deficiency in bone marrow-derived dendritic cells as well as in macrophages isolated from the intraperitoneal cavity of mice, leads to an up-regulation of Arg1 mRNA as well as protein levels (see Figure 12). Arg1 levels were quantified utilizing qPCR as well as western blot analysis (Sahin et al., 2014).

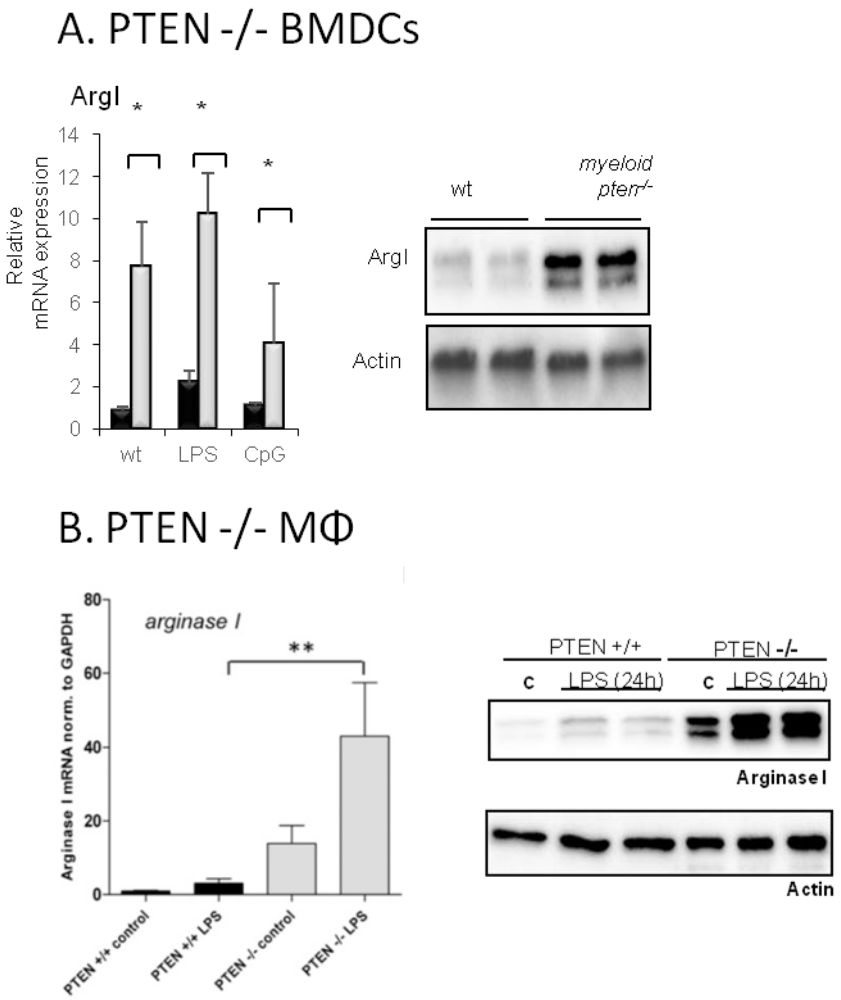


**Figure 12. Arginase 1 is up-regulated in PTEN-deficient bone marrow-derived dendritic cells and macrophages isolated from the intraperitoneal cavity of mice**

A. qPCR and western blot analysis of Arg1 levels of PTEN-deficient as well as wild type bone-marrow derived dendritic cells after stimulation with LPS and CpG. B. mRNA and protein levels of PTEN-deficient and wild type macrophages. Statistical significance is indicated by *P < 0,05.

It has already been shown in previous experiments that the PI3K pathway plays an important role in the fate decision process of macrophages. In line with these findings, our preliminary data show an up-regulation of various M2 markers (Arg, IL-10) as well as a down-regulation of different M1 markers (TNFα and IL-6). Our findings therefore clearly indicate that myeloid PTEN-deficiency leads to a polarization shift in macrophage phenotypes towards the alternatively-activated M2 macrophage phenotype, as can be observed by the change of expression profiles, shown in our preliminary data.

## 4.5 Myeloid PTEN knockout leads to an increase of M2 marker genes in an AOM/DSS driven mouse model of colitis-associated colon cancer

As has been shown in multiple studies, macrophages can contribute to tumor progression, by undergoing phenotypical conversion from the M1 pro-inflammatory, to the M2 tumor-tolerating state. In this study we were interested in verifying, whether this phenomenon also occurs during the course of inflammation driven colon cancer. We therefore used an AOM/DSS driven mouse model of colitis-associated colon cancer, to test if the predicted conversion has effects on tumor growth and progression. We analyzed splenocytes and cells isolated from the mesenteric lymph nodes of myeloid PTEN-deficient mice and wild type control mice, treated with AOM and DSS according to the protocol found in Table 5. To screen for M2 markers we performed quantitative real-time PCR and normalized expression levels to HPRT. Whole tissue homogenates of spleens and mesenteric lymph nodes were generated and used for qPCR in order to screen for the M2 markers Arg1 and Fizz1. As indicated in Figure 13, we found an up-regulation of Arg1 and Fizz1 in the spleen, as well as in the mesenteric lymph node of myeloid PTEN-deficient mice. In line with our hypothesis, this suggests a general preference of PTEN-deficient macrophage to differentiation towards the M2 phenotype during the course of inflammation driven colon cancer (Biswas and Mantovani, 2010).

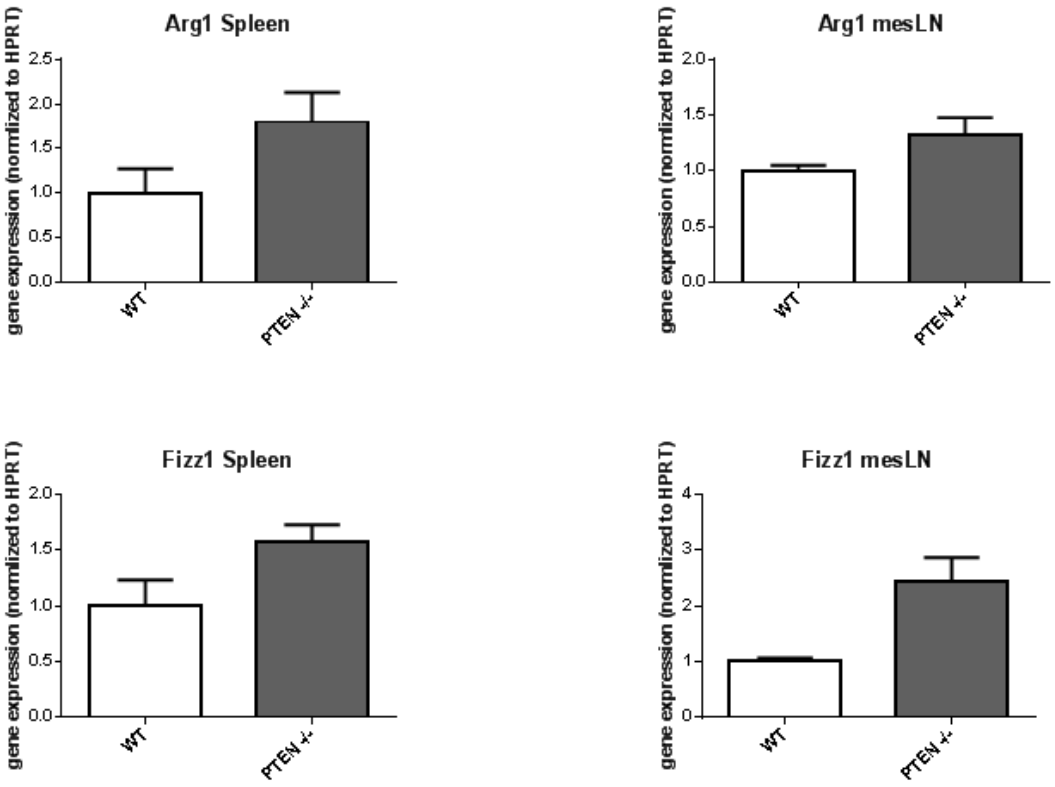


**Figure 13. Myeloid PTEN-deficiency leads to an up-regulation of the M2 markers Arginase 1 and Fizz 1 in the spleen and the mesenteric lymph node.** Expression levels of Arg1 and Fizz 1 in splenocytes and cells isolated from the mesenteric lymph nodes of wild type and myeloid PTEN-deficient mice. Expression levels of mRNA are normalized to HPRT.

As indicated in Figure 13, we found a non-significant tendency of Arg1 and Fizz1 up-regulation in the spleen and the mesenteric lymph node of myeloid PTEN-deficient mice.

Furthermore we were interested in finding out, whether our myeloid PTEN knockout has different effects on CD11b+ and CD11c+ cells. Therefore we isolated CD11b+ and CD11c+ cells from single cell suspension of tissue homogenates obtained from the mice's spleen. This was achieved by the use of magnetic beads. Afterwards we determined mRNA levels of the M2 markers Ym1 and Fizz 1 via quantitative real-time PCR and normalized expression levels to HPRT (see Figure 14).

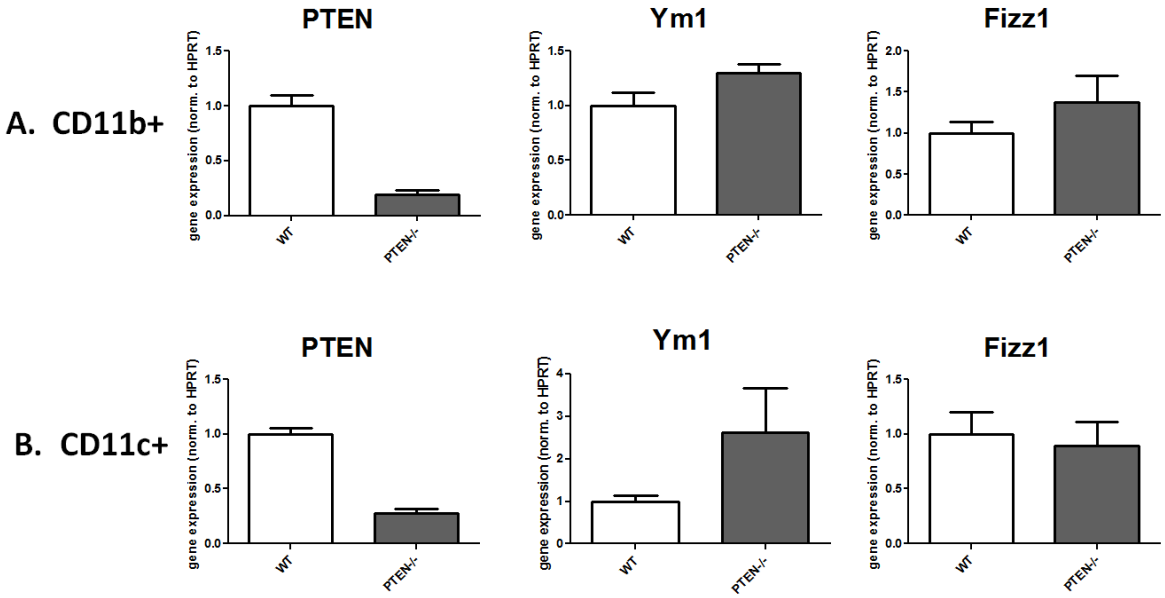


**Figure 14. Myeloid PTEN-deficiency leads to an up-regulation of M2 markers in CD11b+ and CD11c+ cells**

A. Expression levels of PTEN, YM1 and Fizz1 in CD11b+ splenocytes isolated from myeloid PTEN-deficient and wild type mice. B. PTEN, YM1 and Fizz1 expression levels of splenocytes isolated from myeloid PTEN-deficient and wild type mice. Expression levels of mRNA are normalized to HPRT.

As indicated in Figure 14, CD11b+ cells isolated from spleens of myeloid PTEN knockout mice and wild type mice show a strong decrease of PTEN due to the $PTEN^{fl/fl}$ LysM cre knockout. The M2 markers Ym1 and Fizz1 seem to be slightly increased in cells isolated from PTEN -/- compared with the control group. In CD11c+ cells, we also see a drastic decrease of PTEN and an up-regulation of the M2 marker Ym1. In this particular experiment, we could not detect a difference in Fizz1 expression in CD11c+ cells isolated from knockout mice compared with wild type littermate control mice.

## 4.6 Myeloid PTEN-deficiency influences cytokine expression levels in an AOM/DSS driven mouse model of colitis-associated colon cancer

We were also interested in the expression levels of cytokines specific for the M1 and the M2 phenotype. Therefore we performed quantitative real-time PCR with CD11b+ and CD11c+ cells isolated from single cell suspensions of spleens obtained from myeloid PTEN-deficient mice as well as wild type control mice. We then determined the mRNA expression levels of IL-10 and IL-23 in CD11b+ and CD11c+ cells from PTEN-deficient mice versus wild type mice. Interestingly we found a more prominent polarization shift towards the M2 phenotype in CD11c+ dendritic cells. The M2 cytokine IL-10 is up-regulated in PTEN-deficient cells, while expression of the pro-inflammatory M1 cytokine IL-23 is decreased (see Figure 15). As shown in Figure 15, no clear polarization shift was detected in CD11b+ cells in this particular experiment.

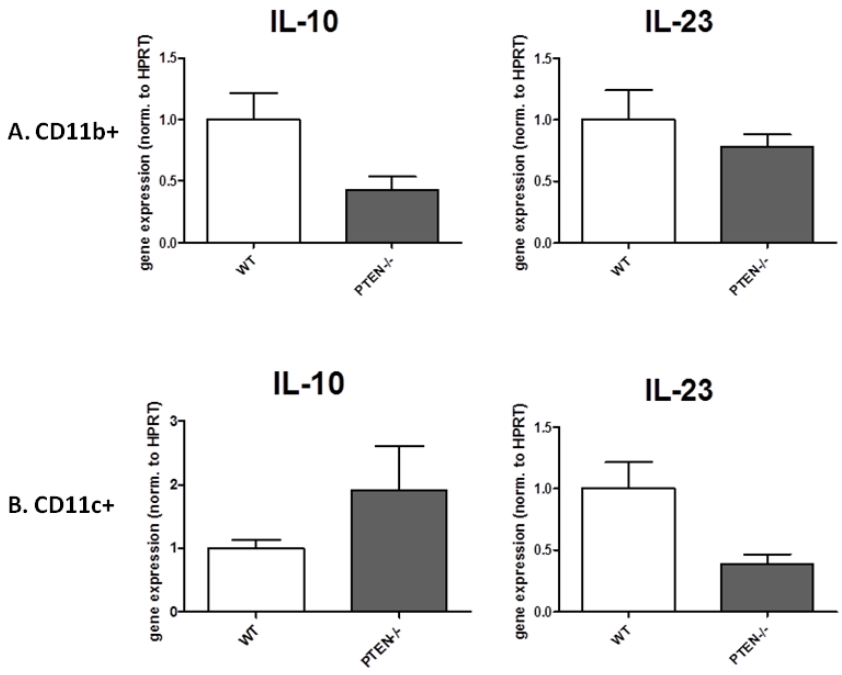


**Figure 15. Myeloid PTEN-deficiency influences cytokine expression levels in an AOM/DSS driven mouse model of colitis-associated colon cancer.** A. Expression levels of IL-10 and IL-23 in CD11b+ splenocytes B. IL-10 and IL-23 mRNA levels in CD11c+ splenocytes. Expression levels of mRNA are normalized to HPRT

Figure 15B clearly indicates a polarization shift towards the M2 phenotype in CD11c+ cells. Therefore we wanted to further investigate this phenotype by looking more closely at CD11c+ dendritic cells.

## 4.7 Myeloid PTEN-deficiency induces hyporesponsiveness in T-cells

As dendritic cells are specialised on the presentation of antigen to T-cells, we wanted to check whether CD11c+ cells isolated from spleens of myeloid PTEN-deficient mice show a difference in their ability to present antigen and activate T-cells. Therefore we performed a T-cell proliferation assay (see Figure 16) and compared cytokine expression levels of CD4+ T-cells isolated from myeloid PTEN knockout mice, with cells isolated from littermate control mice (see Figure 17). T-cell proliferation of total anti-CD3 restimulated CD4+ T-cells from spleens of wild type ($PTEN^{fl/fl}$ LysM cre-) and knockout ($PTEN^{fl/fl}$ LysM cre+) mice after induction of colon cancer by AOM/DSS treatment was analyzed via the quantification of [$^3$H]thymidine incorporation.

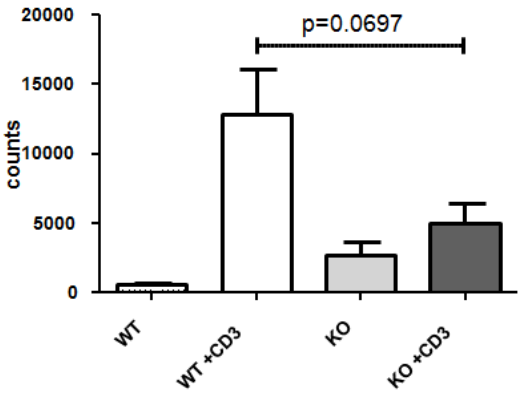


**Figure 16. Myeloid PTEN-deficiency decreases proliferative capacities of CD4+ T-cells**

Proliferation of anti-CD3 restimulated CD4+ T-cells was measured by the quantification of [$^3$H]thymidine incorporation. White bars indicate T-cells isolated from wild type control mice, black bars represent CD4+ cells isolated from myeloid PTEN-deficient mice

As visualized in Figure 16, the proliferative potential of T-cells isolated from spleens of myeloid PTEN-deficient mice, is lower compared with CD4+ cells from wild type littermate

controls. We therefore hypothesize that PTEN-deficient CD11c+ cells have a decreased ability to either present antigen to T-cells or to activate T-cells. Corresponding to this finding, we analyzed cytokine levels produced from CD4+ cells isolate from spleens of myeloid PTEN-deficient mice and compared them to cytokine secretion levels of T-cells isolated from spleens of littermate control mice (see Figure 17).

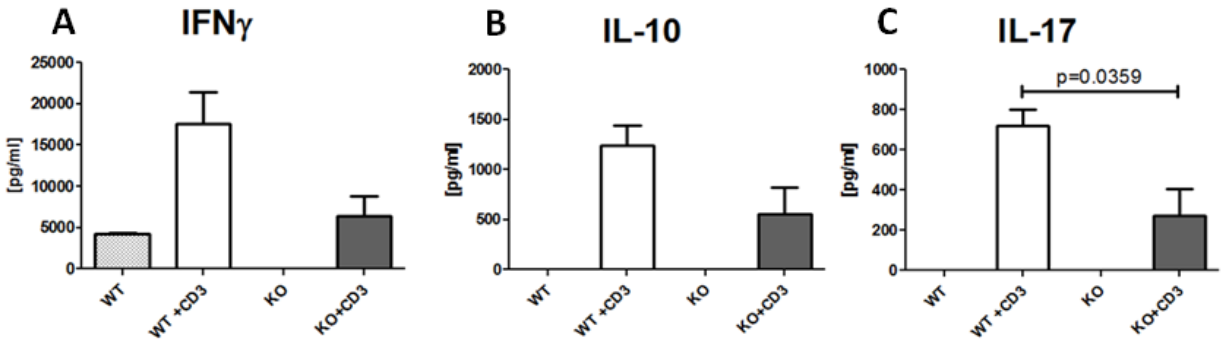


**Figure 17. Myeloid PTEN-deficiency leads to decreased levels of cytokine secretion of CD4+ T-cells**

Secretion levels of IFNγ (A), IL-10 (B) and IL-17(C) [pg/ml] were measured in supernatants of CD4+ T-cells restimulated with anti- CD3 via ELISA analysis

As indicated in Figure 17, the amounts of cytokines produced by CD4+ cells isolated from spleens of myeloid PTEN-deficient mice restimulated with anti-CD3, are in general decreased compared to anti-CD3 restimulated CD4+ T-cells isolated from spleens of wild type mice. The amounts of IFNγ, IL-10 as well as IL-17 seem to be lower in T-cells isolated from myeloid PTEN-knockout ($PTEN^{fl/fl}$ LysM cre+) mice. We speculate that the reason for this finding, is the decreased ability of myeloid PTEN-deficient CD11c+ dendritic cells to activate CD4+ T-cells via antigen presentation. This probably being a consequence of their M2-like immunosuppressive phenotype (see 1.4). Together with the results of the performed [3H]Thymidine proliferation assay, our data suggests a general state of hyporesponsiveness of T-cells induced in myeloid PTEN-knockout mice.

## 4.8 Myeloid PTEN knockout leads to an increase of splenic myeloid-derived suppressor cells (MDSCs)

Myeloid-derived suppressor cells represent a heterogeneous population of Gr1+, CD11b+ myeloid precursor cells that have been shown to expand during the course of various diseases, including cancer, inflammation and infection. By their ability to negatively regulate T-cell functions by direct interaction as well as secreted components, they cause suppressive effects on adaptive immune responses (Gabrilovich and Nagaraj, 2009). To analyze the MDSC populations in our colitis-associated colon cancer mouse model, we used flow cytometry analysis to screen for Gr1+ and Cd11b+ cells in the spleens of myeloid PTEN-knockout mice and wild type mice treated with AOM and DSS to induce colitis-associated colon cancer. As indicated in Figure 18, we found highly increased numbers of Gr1+ and Cd11b+ cells in our knockout mice.

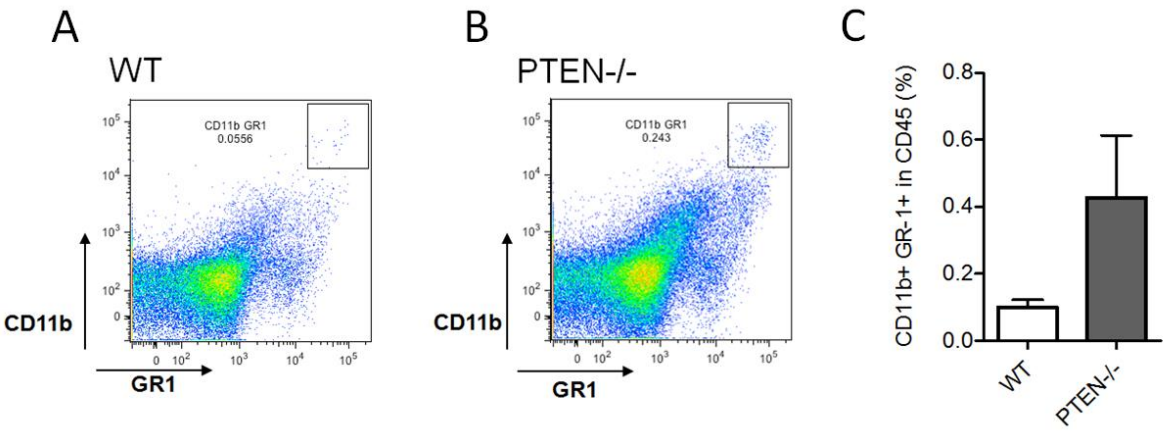


**Figure 18. Myeloid PTEN-deficiency leads to an increase of MDSCs**

A. CD45+ cells of wild type mice were separated according to their CD11b/GR1 expression using FACS analysis B. Cd45+ cells of myeloid PTEN-knockout mice separated by their expression of CD11b and GR1. C. Comparison of CD11b/GR1 positive cells in wild type and knockout mice

## 4.9 Myeloid PTEN-deficiency results in increased tumor burden in an AOM/DSS driven mouse model of colitis-associated colon cancer

To analyze tumor numbers and sizes, colonic tumors were isolated after the AOM/DSS treatment period. To quantify tumor numbers and size, the colon was isolated and arranged in a colonic swiss role (see Figure 9). Organs were fixed with paraformaldehyde and embedded into paraffin blocks to proceed with haematoxylin and eosin (H&E) staining. Hematoxylin results in blue staining of cell nuclei by the interaction of haematoxylin with DNA. A counterstaining with eosin is used to stain the cytoplasm of cells, as well as extracellular proteins such as collagen, in different shades of red and pink. A Tissuefax microscope was used to scan stained colonic tissue sections to quantify tumor numbers, areas and sizes with Histoquest image analysis software (see Figure 19,20).

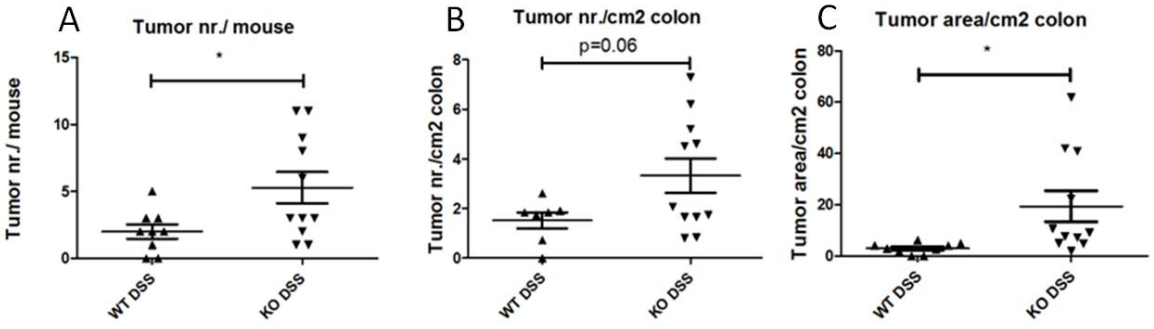


**Figure 19. Myeloid PTEN-deficiency increases tumor burden in an AOM/DSS driven mouse model of colitis-associated colon cancer** A. Tumor number per mouse is significantly increased in myeloid PTEN knockout mice B. Tumor number per $cm^2$ of colon is increased in myeloid PTEN-deficient mice C. Tumor area per $cm^2$ of colon is significantly increased in myeloid PTEN knockout mice. Tumor number and size was normalized to the overall area of the colon. Obtained data were generated by analysis of tissue sections using Histoquest software and results were evaluated using GraphPad Prism software. Statistical significance is indicated by *P < 0,05

As shown in Figure 19, myeloid PTEN-knockout mice are more susceptible to the development of colonic tumors during the AOM/DSS treatment period, compared to wild type littermate controls. The tumor number per mouse is significantly higher in myeloid PTEN-deficient mice, but also the tumor number per $cm^2$ of colon as well as the tumor area per $cm^2$ of colon is increased. This results in an overall elevated tumor burden in our myeloid

PTEN-knockout (PTEN$^{fl/fl}$ LysM cre+) mice. The increased tumor formation in myeloid PTEN-knockout mice is distinctly visible in H&E stained sections of colonic swiss roles (see Figure 20).

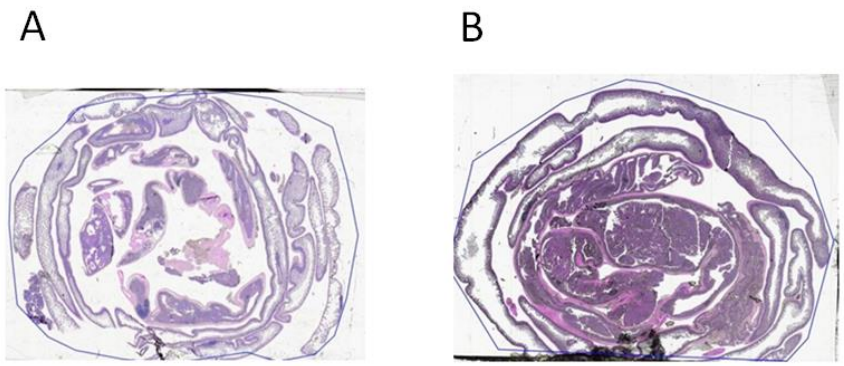


**Figure 20. Myeloid PTEN-deficiency leads to increased tumor formation**

A. H&E stained colon section of AOM/DSS treated wild type mouse B. H&E stained colon section of AOM/DSS treated myeloid PTEN-deficient mouse

Increased tumor incidences, numbers and areas indicated in Figure 19. Are visualized in the histopathological colonic H&E stains presented in Figure 20. Colonic neoplasms developed in myeloid PTEN-deficient mice can easily be observed.

## 4.10 DSS/AOM- treatment leads to weight loss in myeloid PTEN-deficient mice as well as wild type mice

Oral administration of dextran sodium sulphate (DSS) by addition of DSS into the mice's drinking water, is commonly used to mimic human IBD. Previous studies have already shown that DSS treatment leads to diarrhea and weight loss in treated mice. Throughout our experiments, diarrhea of varying severity and weight changes were universally observed (see Figure 21). As indicated in the graph, each cycle of DSS treatment is accompanied by weight loss. A significant difference in the amount of weight loss in DSS treated myeloid PTEN-knockout mice compared with DSS treated wild type mice was not found. Nor did we find a correlation between the amount of weight loss and the stage of tumor progression. However, mice not treated with AOM and DSS but with a single injection of NaCl were not affected by the weight changes.

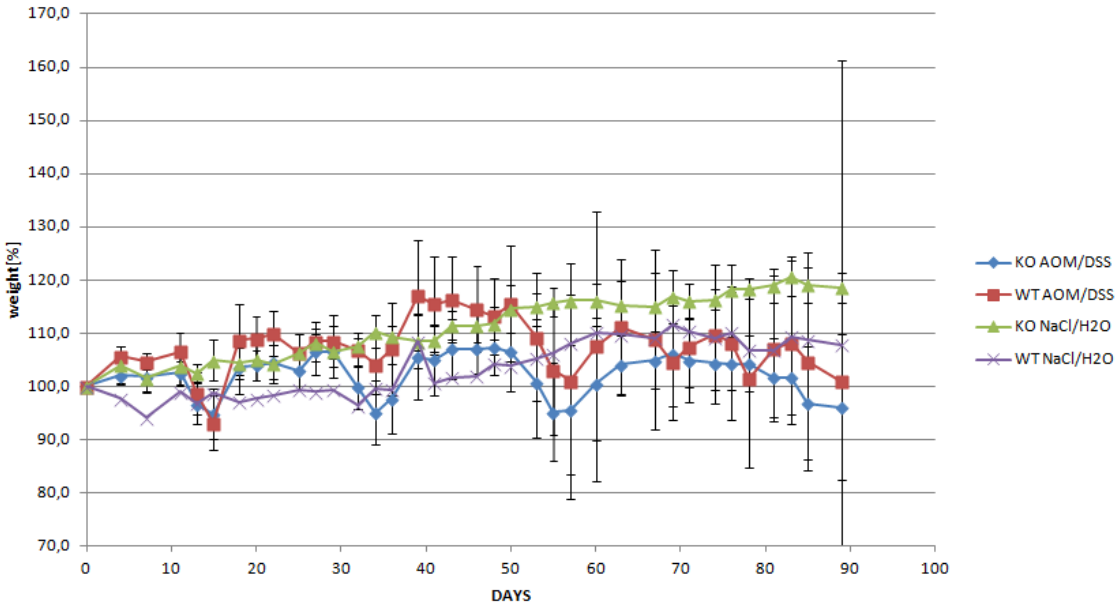


**Figure 21. DSS/AOM- treatment leads to weight loss in wild type as well as PTEN-knockout mice**

KO (knockout) mice as well as WT (wild type) mice, lose weight during the AOM/DSS treatment period, control mice treated with NaCl and water instead gained weight during the experimental period; blue curve shows weight of knockout mice, red curve shows weight of wild type mice treated with AOM and DSS, green curve represents knockout mice, purple curve wild type mice treated with NaCl and $H_20$; error bars indicate standard deviation of mean

## 4.11 Myeloid PTEN-deficiency leads to decreased survival in an AOM/DSS driven mouse model of colitis-associated colon cancer

As a consequence of the immunosuppressive phenotype observed in a variety of PTEN-deficient immune cells, myeloid PTEN-deficient mice are more susceptible to AOM/DSS treatment, which makes them more prone to develop malignant neoplasms. Altogether this results in the phenotype shown in Figure 22, showing a decreased survival of myeloid PTEN-deficient mice during the course of the AOM/DSS treatment period.

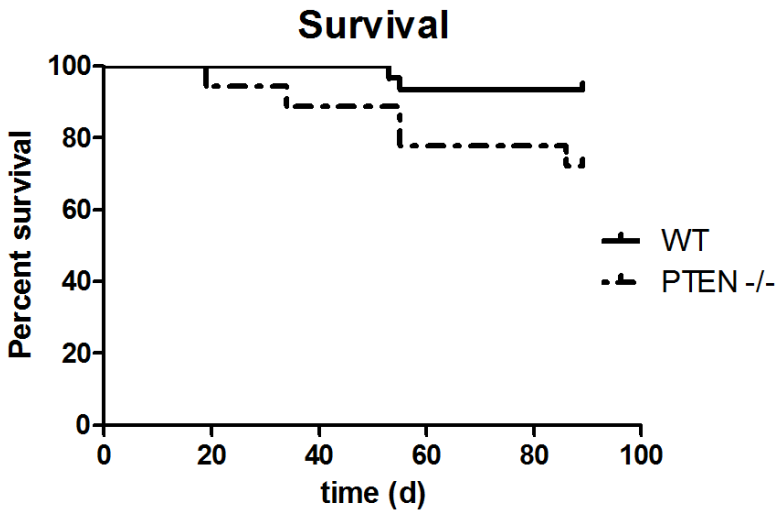


**Figure 22. Survival of myeloid PTEN-deficient and wild type mice during treatment period**

Myeloid PTEN-deficient mice (perforated line) show a decreased survival during the time course of the experiment, when compared to wild type mice (continuous line); male mice are shown

# 5. Discussion

Previous studies of our group have focused on the role of myeloid PTEN in a murine model for multiple sclerosis: experimental autoimmune encephalomyelitis (EAE) (Sahin et al., 2014). In this context we showed that myeloid PTEN plays an important role in the susceptibility to inflammation and that myeloid PTEN-deficiency positively influences Arginase 1 (Arg1) expression, indicating a polarization shift of macrophages towards the M2 phenotype (Biswas and Mantovani, 2010). In this study we focus on the role of the PTEN pathway in myeloid cells in tumor immune surveillance in an AOM/DSS driven mouse model of colitis-associated colon cancer (CAC).

Therefore we induced CAC in myeloid PTEN-knockout and wild type mice, using a conditional knockout system, in which the expression of cre recombinase is dependent on the activity of the Lysozyme M (LysM) promoter. Lysozyme is a secretory product of phagocytes, but is also found in the granules of granulocytes. Therefore our knockout system mostly targets peripheral monocytes, macrophages and tissue resident macrophages. However, granulocytes and some dendritic cell subsets can also be affected. Previous studies suggest that the LysM promoter does not allow discrimination between different types of myeloid cell subsets, but propose that LysM is expressed to a smaller extend in CD11c+ dendritic cells compared to other CD11b expressing cell subsets (Hume, 2011). This is probably due to the fact that even though macrophages and dendritc cells are both able to present antigens and phagocytose microbes, dendritic cells are specialized on the presentation of antigen rather than phagocytosis, whereas macrophages are the major phagocytic cells. Therefore we use this knockout system to characterize myeloid PTEN-deficient macrophages, but are aware of the fact that we might also target other myeloid cell subpopulations.

To trigger CAC in myeloid PTEN-deficient mice, we used an AOM/DSS model, where dextran sodium sulphate is used to mimic inflammatory bowel disease (Okayasu et al., 1990; Seril et al., 2002). In order to establish CAC, mice were pretreated with a single injection of the genotoxic colonic carcinogen Azoxymethan (AOM), which causes DNA damage by alkylation.

We found that repeated administration of DSS into the drinking water of the mice, results in weight loss, shortening of the colon, as well as diarrhea. Furthermore DSS treatment led to the development of colonic tumors, when combined with an intraperitoneal injection of AOM at the start of the experiment.

We show that myeloid PTEN-deficiency influences a variety of cell-types of the innate- as well as the adaptive immune system of myeloid and lymphoid origin during the course of AOM/DSS treatment. Tumor cells have the ability to actively recruit macrophages by the secretion of various cytokines and chemokins. The fate of recruited macrophages is then determined by the tumors microenvironment. While an IFNγ (produced by $T_H1$ cells) rich environment promotes classical activation of macrophages, skewing them towards an M1 phenotype, the presence of IL-4 (produced by $T_H2$ cells) polarizes macrophages towards an M2 phenotype. Over the course of tumor progression, macrophages in general switch from M1 to M2-like properties. Alternatively activated macrophages usually show a tumor-tolerating, immune-suppressive phenotype. They are involved in the promotion of $T_H2$ response, decrease inflammation, encourage tissue repair and wound healing and are characterized by the up-regulation of a variety of marker genes including Arginase 1 (Arg1), Fizz1 and Ym1 (Biswas and Mantovani, 2010). Consistent with previous experiments performed with $PTEN^{fl/fl}$ LysM cre+ mice, we show that myeloid PTEN-deficiency leads to an up-regulation of M2 marker genes in splenocytes isolated from knockout mice.

Preliminary experiments performed with myeloid PTEN-knockout mice in a murine model for multiple sclerosis (EAE), already showed that myeloid PTEN-deficiency positively influences Arginase 1 expression. Significantly higher levels of Arg1 mRNA- as well as protein levels were detected in PTEN-deficient bone-marrow derived dendritic cells, as well as PTEN-deficient intraperitoneal macrophages, after stimulation with LPS or CpG. Furthermore, myeloid PTEN-deficient macrophages showed increased mRNA- as well as cytokine-secretion levels of the M2 cytokine IL-10 after LPS stimulation when compared to wild type macrophages. Decreased mRNA levels of the pro-inflammatory cytokines IL-6 and TNFα were detected in macrophages isolated from the intraperitoneal cavity of myeloid PTEN-deficient mice, compared to cells isolated from littermate control mice.

In line with the transcriptional down-regulation, significantly lower levels of IL-6 and TNFα secreted into the supernatants of cultivated knockout macrophages after their stimulation with a variety of toll-like-receptor-ligands were found (Sahin et al., 2014).

Consistent with these findings, we found that cells isolated from spleens and mesenteric lymph nodes of AOM/DSS treated mice, show increased mRNA levels of Arginase 1. Furthermore we detected an up-regulation of the M2 marker genes Fizz1 and Ym1 on mRNA levels of splenocytes isolated from knockout mice.

When looking at mRNA levels of different cytokines, we found an up-regulation of the anti-inflammatory M2 cytokine IL-10 and a down-regulation of the pro-inflammatory cytokine IL-23. Surprisingly this phenotype was even more prominent in CD11c+ cells when compared to CD11b+ cells, leading to the assumption that dendritic cells play an important role in the observed phenotype. Upon isolation of CD11b+ and CD11c+ cells from splenocytes obtained from myeloid PTEN-deficient as well as wild type mice, we found that PTEN is strongly down-regulated in both cell types. A close examination of the expression profiles of Arg1 and Fizz1, revealed that CD11c+ cells also show increased levels of M2 markers. While the role of dendritic cells during the course of our experiments needs further investigation, we so far conclude that the used knockout system not only targets macrophages, but also dendritic cells.

We therefore asked the question whether dendritic cells isolated from spleens of myeloid PTEN-deficient mice are compromised in their antigen-presenting function or their ability to activate T-cells. By performing T-cell proliferation assays and analyzing cytokine profiles of CD4+ T-cells isolated from wild type and knockout mice, we found that myeloid PTEN-deficiency induces hyporesponsiveness in CD4+ T-cells, isolated from spleens of AOM/DSS treated mice. We showed that T-cell proliferation of anti-CD3 restimulated CD4+ cells, isolated from knockout animals was impaired, compared to cells isolated from littermate wild type controls. Furthermore we found that myeloid PTEN-deficiency leads to decreased levels of cytokines secreted by CD4+ cells. This data suggests that dendritic cells are affected by our knockout system, and that PTEN-deficiency in dendritic cells negatively influences their ability to activate and prime CD4+ cells, probably due to the impaired antigen-presenting ability of PTEN-deficient CD11c+ cells. We plan on repeating these experiments with CD11c+ cells isolated from healthy and cancerous colonic tissue.

FACS analysis of splenocytes isolated from wild type and knockout mice, revealed an increase in myeloid derived suppressor cells in myeloid PTEN-deficient mice. Since MDSCs generally represent a population of myeloid precursor cells, exhibiting an immune-suppressive phenotype by their ability to suppress T-cells, this finding supports our hypothesis that myeloid PTEN-deficiency in mice leads to a decrease of anti-tumor immune responses and an increase in immunosuppression (Gabrilovich and Nagaraj, 2009).

Probably as a result of the up-regulation of immunosuppressive immune cells, we were able to show that myeloid PTEN-deficiency results in increased tumor burden in an AOM/DSS driven mouse model of CAC. Immunohistochemistry of colon sections isolated from myeloid PTEN-deficient, as well as littermate wild type mice treated with AOM and DSS, revealed that knockout mice showed tumors increased in number, size and area, when compared to wild type controls. PTEN-knockout mice are more susceptible to the development of colonic tumors during the AOM/DSS treatment period, show higher tumor numbers and bigger tumors when compared to wild type littermate controls. We assume that the increased tumor burden found in our knockout mice, results from the fact that the PI3K/PTEN pathway plays a crucial role in the fate decision and polarization process of macrophages. Based on mRNA levels of M2 marker genes, which we found to be increased in myeloid cells isolated from knockout animals, we suggest that myeloid PTEN-deficiency leads to a shift in macrophage polarization states towards the alternatively activated M2 macrophage phenotype. We suggest that the increased expression of various M2 markers subsequently leads to a decrease of anti-tumor immune responses and inflammation through various mechanisms which are triggered by the up-regulated expression of these genes. For instance, enhanced expression of Arg1 mRNA, leads to a cellular increase of the corresponding enzyme Arginase1. By catalyzing the reaction from arginine and $H_2O$ to ornithine and urea, consumption of arginine is boosted and can result in a depletion of the amino acid in the surrounding environment of affected cells (Makarenkova et al., 2006; Rodriguez et al., 2003). Through the reduction of available arginine, macrophages can diminish T-cell functions, as T-cells utilize arginine for proliferation, the expression of toll-like-receptors, as well as the development of memory. Arginine is therefore essential for T-cell functions, as they depend on arginine for a variety of biological processes (Bronte et al., 2003; Ochoa et al., 2001).

Concerning the M2 marker Fizz1, a study recently conducted by Osborn et al., demonstrated a pathogenic role of Fizz1 during DSS induced colitis. Their experiments show that Fizz-/- knockout mice are protected from excessive intestinal inflammation after DSS treatment. A correlation between decreased disease severity and reduced expression of IL-17 by CD4+ T-cells was found in those mice, suggesting that increased Fizz1 expression enhances CD4+ T-cell response, thereby increasing inflammation and severity of colitis (Osborne et al., 2013).

Another study recently published by Kawada et al., focuses on the role of YM1 during the course of colorectal cancer. Performed experiments suggest that enhanced expression of YM1 promotes cancer cell proliferation as well as angiogenesis and is generally correlated with poor prognosis in cancer patients (Kawada et al., 2012).

Enhanced expression of the anti-inflammatory cytokine IL-10 has been proposed to influence immune responses through the promotion of regulatory T-cells and the down-regulation of $T_H1$ response, thereby leading to a down-modulation of anti-tumor immune responses (Terzić et al., 2010).

Many mechanisms by which up-regulation of M2 markers influences the immune system are still poorly understood and yet have to be uncovered. However we suggest that by a combination of diverse mechanisms triggered by the up-regulation of M2 markers, alternatively activated myeloid cells lead to the increased susceptibility to tumor development and progression as well as elevated tumor burden in our knockout mice. As a consequence of the observed immunosuppressive phenotype in a multiplicity of PTEN-deficient immune cells, knockout mice are more prone to develop malignant neoplasms during AOM/DSS treatment.

Probably as a result of the increased susceptibility of knockout mice to develop malignant tumors, myeloid PTEN-deficient mice show decreased survival during the course of the AOM/DSS treatment period. However at this point we cannot rule out that myeloid PTEN-deficiency might also lead to an increased susceptibility of knockout mice to infections which could also affect their survival.

In summary the performed experiments, support our initial hypothesis about the role of PI3K as a crucial modulator of the innate immune system. We were able to show that constitutive activation of PI3K in myeloid cells not only affects myeloid cells themselves, but also influences the responsiveness of T-cells. Ablation of PTEN in myeloid cells leads to a down-modulation of the innate immune response, dampening immune properties of macrophages towards colon cancer cells, by skewing macrophages towards an anti-inflammatory, tumor-tolerating M2 phenotype.

Although recent experiments support our hypothesis, many unanswered questions remain. One of our most important goals for the future is to isolate and characterize myeloid cells, obtained from colonic neoplasms and the colon of myeloid PTEN-deficient mice, and analyze

their expression profiles. So far we focused on the investigation of cells isolated from lymphoid organs and now plan to isolate colons of AOM/DSS treated wild type and knockout mice in order to investigate cells found in colonic tumors as well as the tumors' stroma. By analyzing cytokines and mRNA levels of marker genes, we hope to characterize immune cells implicated in tumor immune responses of myeloid PTEN-deficient, as well as wild type mice.

Our data indicates an important role of PI3K in CD11c+ dendritic cells, as CD11c+ cells with enhanced levels of PI3K show a decreased ability to activate T-cells. We currently focus on the analysis of a conditional knockout system, where the expression of cre recombinase is dependent on the activity of the CD11c promoter. By the ablation of PI3K in dendritic cells, this model will permit to study of the role of the PI3K/PTEN pathway directly in CD11c+ dendritic cells.

# 6. List of Figures

# 7. List of tables

# 8. Curriculum Vitae

Leslie Hanzl
E-Mail: Leslie.Hanzl@gmx.at

**Personal Information:**

Citizenship: Austria
Family status: unmarried

**Education:**

| | |
|---|---|
| since 2012: | Master studies of genetics and molecular pathology at the university of Vienna, sponsorship for outstanding performances |
| | Completion of Master studies and receipt of Masters' degree of Science (MSc): June 2015 |
| since 2008: | Bachelor studies of genetics and microbiology at the university of Vienna, sponsorship for outstanding performances |
| | March 2013: receipt of Bachelors' degree of Science (BSc) |
| 1999-2007: | Secondary school "Untere Bachgasse 8, Mödling", focus on Biology and Chemistry |
| | June 2007: graduation with superior success |

**Experiences:**

April 2014 – April 2015:
Full-time deployment at the Medical University of Vienna as a Mater student at the Institute of Physiology and Pharmacology

June 2013 – September 2013:
Part-time Deployment as a salesperson at bbo plus Berufsmoden, Guntramsdorf

March 2012 – August 2012:
Internship and part-time deployment at the department of chromosomal biology at the Institute of Molecular Biotechnology of the Austrian Academy of Science (IMBA) in Vienna

Since 2008:
Regular practical courses and internships in the fields of molecular biology,

| | |
|---|---|
| | microbiology, genetics, developmental biology and cytogenetics, light- and konfocal – microscopy, etc. |
| | May 2008 – January 2009: waitress in an Austrian vinery |
| | September 2007 – April 2008:<br>Language stay in Australia, successful completion of the Cambridge Certificate of Advanced English |
| | July 2005: internship at easybank Vienna |
| **Special skills:** | Excellent English language skills |
| | Basic knowledge of French |
| | Driving licence since August 2006 |
| **Computer skills:** | Very good knowledge of Microsoft Word and Excel, basic knowledge of Adobe Photoshop |
| | Experience in working with biological sequence- and protein-databases |
| | Experience with microscopy software (e.g. konfocal microscopy software) |
| **Hobbies:** | Life science |
| | Teamwork and group-activities (participation and work as a member of the scouts for ten years) |
| | Photography |
| | Acting |

# 9. References


Atreya, I., and M. F. Neurath, 2008, Immune cells in colorectal cancer: prognostic relevance and therapeutic strategies: Expert Rev Anticancer Ther, v. 8, p. 561-72.

Barker, N., R. A. Ridgway, J. H. van Es, M. van de Wetering, H. Begthel, M. van den Born, E. Danenberg, A. R. Clarke, O. J. Sansom, and H. Clevers, 2009, Crypt stem cells as the cells-of-origin of intestinal cancer: Nature, v. 457, p. 608-11.

Barker, N., J. H. van Es, J. Kuipers, P. Kujala, M. van den Born, M. Cozijnsen, A. Haegebarth, J. Korving, H. Begthel, P. J. Peters, and H. Clevers, 2007, Identification of stem cells in small intestine and colon by marker gene Lgr5: Nature, v. 449, p. 1003-7.

Biswas, S., A. Chytil, K. Washington, J. Romero-Gallo, A. E. Gorska, P. S. Wirth, S. Gautam, H. L. Moses, and W. M. Grady, 2004, Transforming growth factor beta receptor type II inactivation promotes the establishment and progression of colon cancer: Cancer Res, v. 64, p. 4687-92.

Biswas, S. K., and A. Mantovani, 2010, Macrophage plasticity and interaction with lymphocyte subsets: cancer as a paradigm: Nat Immunol, v. 11, p. 889-96.

Biswas, S. K., A. Sica, and C. E. Lewis, 2008, Plasticity of macrophage function during tumor progression: regulation by distinct molecular mechanisms: J Immunol, v. 180, p. 2011-7.

Bottazzi, B., A. Doni, C. Garlanda, and A. Mantovani, 2010, An integrated view of humoral innate immunity: pentraxins as a paradigm: Annu Rev Immunol, v. 28, p. 157-83.

Bowdish, D. M., M. S. Loffredo, S. Mukhopadhyay, A. Mantovani, and S. Gordon, 2007, Macrophage receptors implicated in the "adaptive" form of innate immunity: Microbes Infect, v. 9, p. 1680-7.

Bronte, V., P. Serafini, A. Mazzoni, D. M. Segal, and P. Zanovello, 2003, L-arginine metabolism in myeloid cells controls T-lymphocyte functions: Trends Immunol, v. 24, p. 302-6.

Cantley, L. C., 2002, The phosphoinositide 3-kinase pathway: Science, v. 296, p. 1655-7.

Clausen, B. E., C. Burkhardt, W. Reith, R. Renkawitz, and I. Förster, 1999, Conditional gene targeting in macrophages and granulocytes using LysMcre mice: Transgenic Res, v. 8, p. 265-77.

Clevers, H., and E. Batlle, 2013, SnapShot: the intestinal crypt: Cell, v. 152, p. 1198-1198 e2.

DeNardo, D. G., J. B. Barreto, P. Andreu, L. Vasquez, D. Tawfik, N. Kolhatkar, and L. M. Coussens, 2009, CD4(+) T cells regulate pulmonary metastasis of mammary carcinomas by enhancing protumor properties of macrophages: Cancer Cell, v. 16, p. 91-102.

Eaden, J. A., K. R. Abrams, and J. F. Mayberry, 2001, The risk of colorectal cancer in ulcerative colitis: a meta-analysis: Gut, v. 48, p. 526-35.

Fearon, E. R., S. R. Hamilton, and B. Vogelstein, 1987, Clonal analysis of human colorectal tumors: Science, v. 238, p. 193-7.

Fearon, E. R., and B. Vogelstein, 1990, A genetic model for colorectal tumorigenesis: Cell, v. 61, p. 759-67.

Gabrilovich, D. I., and S. Nagaraj, 2009, Myeloid-derived suppressor cells as regulators of the immune system: Nat Rev Immunol, v. 9, p. 162-74.

Geissmann, F., S. Gordon, D. A. Hume, A. M. Mowat, and G. J. Randolph, 2010, Unravelling mononuclear phagocyte heterogeneity: Nat Rev Immunol, v. 10, p. 453-60.

Gordon, S., and P. R. Taylor, 2005, Monocyte and macrophage heterogeneity: Nat Rev Immunol, v. 5, p. 953-64.

Grady, W. M., and J. M. Carethers, 2008, Genomic and epigenetic instability in colorectal cancer pathogenesis: Gastroenterology, v. 135, p. 1079-99.

Gunzl, P., and G. Schabbauer, 2008, Recent advances in the genetic analysis of PTEN and PI3K innate immune properties: Immunobiology, v. 213, p. 759-65.

Gupta, R. A., and R. N. Dubois, 2001, Colorectal cancer prevention and treatment by inhibition of cyclooxygenase-2: Nat Rev Cancer, v. 1, p. 11-21.

Günzl, P., K. Bauer, E. Hainzl, U. Matt, B. Dillinger, B. Mahr, S. Knapp, B. R. Binder, and G. Schabbauer, 2010, Anti-inflammatory properties of the PI3K pathway are mediated by IL-10/DUSP regulation: J Leukoc Biol, v. 88, p. 1259-69.

Günzl, P., and G. Schabbauer, 2008, Recent advances in the genetic analysis of PTEN and PI3K innate immune properties: Immunobiology, v. 213, p. 759-65.

Hazlett, L. D., S. A. McClellan, R. P. Barrett, X. Huang, Y. Zhang, M. Wu, N. van Rooijen, and E. Szliter, 2010, IL-33 shifts macrophage polarization, promoting resistance against Pseudomonas aeruginosa keratitis: Invest Ophthalmol Vis Sci, v. 51, p. 1524-32.

Hollander, M. C., G. M. Blumenthal, and P. A. Dennis, 2011, PTEN loss in the continuum of common cancers, rare syndromes and mouse models: Nat Rev Cancer, v. 11, p. 289-301.

Hume, D. A., 2011, Applications of myeloid-specific promoters in transgenic mice support in vivo imaging and functional genomics but do not support the concept of distinct macrophage and dendritic cell lineages or roles in immunity: J Leukoc Biol, v. 89, p. 525-38.

Johansson, M. E., J. K. Gustafsson, K. E. Sjöberg, J. Petersson, L. Holm, H. Sjövall, and G. C. Hansson, 2010, Bacteria penetrate the inner mucus layer before inflammation in the dextran sulfate colitis model: PLoS One, v. 5, p. e12238.

Kawada, M., H. Seno, K. Kanda, Y. Nakanishi, R. Akitake, H. Komekado, K. Kawada, Y. Sakai, E. Mizoguchi, and T. Chiba, 2012, Chitinase 3-like 1 promotes macrophage recruitment and angiogenesis in colorectal cancer: Oncogene, v. 31, p. 3111-23.

Kusmartsev, S., Y. Nefedova, D. Yoder, and D. I. Gabrilovich, 2004, Antigen-specific inhibition of CD8+ T cell response by immature myeloid cells in cancer is mediated by reactive oxygen species: J Immunol, v. 172, p. 989-99.

Lakatos, P. L., and L. Lakatos, 2008, Risk for colorectal cancer in ulcerative colitis: changes, causes and management strategies: World J Gastroenterol, v. 14, p. 3937-47.

Makarenkova, V. P., V. Bansal, B. M. Matta, L. A. Perez, and J. B. Ochoa, 2006, CD11b+/Gr-1+ myeloid suppressor cells cause T cell dysfunction after traumatic stress: J Immunol, v. 176, p. 2085-94.

Mantovani, A., 2008, From phagocyte diversity and activation to probiotics: back to Metchnikoff: Eur J Immunol, v. 38, p. 3269-73.

Mantovani, A., P. Allavena, A. Sica, and F. Balkwill, 2008a, Cancer-related inflammation: Nature, v. 454, p. 436-44.

Mantovani, A., P. Romero, A. K. Palucka, and F. M. Marincola, 2008b, Tumour immunity: effector response to tumour and role of the microenvironment: Lancet, v. 371, p. 771-83.

Mantovani, A., A. Sica, S. Sozzani, P. Allavena, A. Vecchi, and M. Locati, 2004, The chemokine system in diverse forms of macrophage activation and polarization: Trends Immunol, v. 25, p. 677-86.

Mantovani, A., S. Sozzani, M. Locati, P. Allavena, and A. Sica, 2002, Macrophage polarization: tumor-associated macrophages as a paradigm for polarized M2 mononuclear phagocytes: Trends Immunol, v. 23, p. 549-55.

Martinez, F. O., S. Gordon, M. Locati, and A. Mantovani, 2006, Transcriptional profiling of the human monocyte-to-macrophage differentiation and polarization: new molecules and patterns of gene expression: J Immunol, v. 177, p. 7303-11.

Morin, P. J., A. B. Sparks, V. Korinek, N. Barker, H. Clevers, B. Vogelstein, and K. W. Kinzler, 1997, Activation of beta-catenin-Tcf signaling in colon cancer by mutations in beta-catenin or APC: Science, v. 275, p. 1787-90.

Mosser, D. M., and J. P. Edwards, 2008, Exploring the full spectrum of macrophage activation: Nat Rev Immunol, v. 8, p. 958-69.

Ochoa, J. B., J. Strange, P. Kearney, G. Gellin, E. Endean, and E. Fitzpatrick, 2001, Effects of L-arginine on the proliferation of T lymphocyte subpopulations: JPEN J Parenter Enteral Nutr, v. 25, p. 23-9.

Oguma, K., H. Oshima, M. Aoki, R. Uchio, K. Naka, S. Nakamura, A. Hirao, H. Saya, M. M. Taketo, and M. Oshima, 2008, Activated macrophages promote Wnt signalling through tumour necrosis factor-alpha in gastric tumour cells: EMBO J, v. 27, p. 1671-81.

Okayasu, I., S. Hatakeyama, M. Yamada, T. Ohkusa, Y. Inagaki, and R. Nakaya, 1990, A novel method in the induction of reliable experimental acute and chronic ulcerative colitis in mice: Gastroenterology, v. 98, p. 694-702.

Osborne, L. C., K. L. Joyce, T. Alenghat, G. F. Sonnenberg, P. R. Giacomin, Y. Du, K. S. Bergstrom, B. A. Vallance, and M. G. Nair, 2013, Resistin-like molecule α promotes pathogenic Th17 cell responses and bacterial-induced intestinal inflammation: J Immunol, v. 190, p. 2292-300.

Oshima, M., J. E. Dinchuk, S. L. Kargman, H. Oshima, B. Hancock, E. Kwong, J. M. Trzaskos, J. F. Evans, and M. M. Taketo, 1996, Suppression of intestinal polyposis in Apc delta716 knockout mice by inhibition of cyclooxygenase 2 (COX-2): Cell, v. 87, p. 803-9.

Peyssonnaux, C., V. Datta, T. Cramer, A. Doedens, E. A. Theodorakis, R. L. Gallo, N. Hurtado-Ziola, V. Nizet, and R. S. Johnson, 2005, HIF-1alpha expression regulates the bactericidal capacity of phagocytes: J Clin Invest, v. 115, p. 1806-15.

Podolsky, D. K., 2002, Inflammatory bowel disease: N Engl J Med, v. 347, p. 417-29.

Raes, G., L. Brys, B. K. Dahal, J. Brandt, J. Grooten, F. Brombacher, G. Vanham, W. Noël, P. Bogaert, T. Boonefaes, A. Kindt, R. Van den Bergh, P. J. Leenen, P. De Baetselier, and G. H. Ghassabeh, 2005, Macrophage galactose-type C-type lectins as novel markers for alternatively activated macrophages elicited by parasitic infections and allergic airway inflammation: J Leukoc Biol, v. 77, p. 321-7.

Rodriguez, P. C., A. H. Zea, J. DeSalvo, K. S. Culotta, J. Zabaleta, D. G. Quiceno, J. B. Ochoa, and A. C. Ochoa, 2003, L-arginine consumption by macrophages modulates the expression of CD3 zeta chain in T lymphocytes: J Immunol, v. 171, p. 1232-9.

Rubinfeld, B., B. Souza, I. Albert, O. Müller, S. H. Chamberlain, F. R. Masiarz, S. Munemitsu, and P. Polakis, 1993, Association of the APC gene product with beta-catenin: Science, v. 262, p. 1731-4.

Sahin, E., S. Haubenwallner, M. Kuttke, I. Kollmann, A. Halfmann, A. M. Dohnal, A. B. Dohnal, L. Chen, P. Cheng, B. Hoesel, E. Einwallner, J. Brunner, J. B. Kral, W. C. Schrottmaier, K. Thell, V. Saferding, S. Blüml, and G. Schabbauer, 2014, Macrophage PTEN regulates expression and secretion of arginase I modulating innate and adaptive immune responses: J Immunol, v. 193, p. 1717-27.

Schneikert, J., and J. Behrens, 2007, The canonical Wnt signalling pathway and its APC partner in colon cancer development: Gut, v. 56, p. 417-25.

Seril, D. N., J. Liao, K. L. Ho, A. Warsi, C. S. Yang, and G. Y. Yang, 2002, Dietary iron supplementation enhances DSS-induced colitis and associated colorectal carcinoma development in mice: Dig Dis Sci, v. 47, p. 1266-78.

Sica, A., and A. Mantovani, 2012, Macrophage plasticity and polarization: in vivo veritas: J Clin Invest, v. 122, p. 787-95.

Sinha, P., V. K. Clements, S. K. Bunt, S. M. Albelda, and S. Ostrand-Rosenberg, 2007, Cross-talk between myeloid-derived suppressor cells and macrophages subverts tumor immunity toward a type 2 response: J Immunol, v. 179, p. 977-83.

Suzuki, A., M. T. Yamaguchi, T. Ohteki, T. Sasaki, T. Kaisho, Y. Kimura, R. Yoshida, A. Wakeham, T. Higuchi, M. Fukumoto, T. Tsubata, P. S. Ohashi, S. Koyasu, J. M. Penninger, T. Nakano, and T. W. Mak, 2001, T cell-specific loss of Pten leads to defects in central and peripheral tolerance: Immunity, v. 14, p. 523-34.

Takaku, K., M. Oshima, H. Miyoshi, M. Matsui, M. F. Seldin, and M. M. Taketo, 1998, Intestinal tumorigenesis in compound mutant mice of both Dpc4 (Smad4) and Apc genes: Cell, v. 92, p. 645-56.

Tenesa, A., and M. G. Dunlop, 2009, New insights into the aetiology of colorectal cancer from genome-wide association studies: Nat Rev Genet, v. 10, p. 353-8.

Terzić, J., S. Grivennikov, E. Karin, and M. Karin, 2010, Inflammation and colon cancer: Gastroenterology, v. 138, p. 2101-2114.e5.

van Hogezand, R. A., R. F. Eichhorn, A. Choudry, R. A. Veenendaal, and C. B. Lamers, 2002, Malignancies in inflammatory bowel disease: fact or fiction?: Scand J Gastroenterol Suppl, p. 48-53.

Vanhaesebroeck, B., S. J. Leevers, K. Ahmadi, J. Timms, R. Katso, P. C. Driscoll, R. Woscholski, P. J. Parker, and M. D. Waterfield, 2001, Synthesis and function of 3-phosphorylated inositol lipids: Annu Rev Biochem, v. 70, p. 535-602.

Worby, C. A., and J. E. Dixon, 2014, Pten: Annu Rev Biochem, v. 83, p. 641-69.